Wind Turbine Blade Section Optimization Shape Using Improved Genetic Algorithm by Coupling Parameterization

By

Deepak Kumar

Registration No: 00000362796

Department of Energy Systems Engineering

US Pakistan Center for Advanced Studies in Energy (USPCAS-E)

National University of Sciences & Technology (NUST)

Islamabad, Pakistan

(2024)

Wind Turbine Blade Section Optimization Shape Using Improved Genetic Algorithm by Coupling Parameterization

By

Deepak Kumar

(Registration No: 00000362796)

A thesis submitted to the National University of Sciences and Technology, Islamabad,

in partial fulfillment of the requirements for the degree of

Master of Science in
Energy Systems Engineering

Supervisor: Dr. Majid Ali

Co-Supervisor: Dr Sehar Shakir

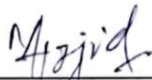US Pakistan Center for Advanced Studies in Energy (USPCAS-E)

National University of Sciences & Technology (NUST)

Islamabad, Pakistan

(2024)

THESIS ACCEPTANCE CERTIFICATE

Certified that final copy of MS Thesis written by Mr. **Deepak Kumar** (Registration No. **00000362796**), of Department of Energy Systems Engineering, School of U.S Pakistan Center for Advanced Studies in Energy, National University of Sciences & Technology (NUST) Islamabad, Pakistan, has been vetted by undersigned, found complete in all respects as per NUST Statutes/ Regulations/ Masters Policy, is free of plagiarism, errors, and mistakes and is accepted as partial fulfillment for award of master's degree. It is further certified that necessary amendments as pointed out by GEC members and foreign/ local evaluators of the scholar have also been incorporated in the said thesis.

Signature: _____

Name of Supervisor: _____Dr. Majid Ali_____

Date: _____19/12/2024_____

Signature (HOD): _____

Date: _____20 -12 - 2024_____

Signature (Dean/ Principal) _____

Date: _____26/12/2024_____

National University of Sciences & Technology
MASTER'S THESIS WORK

We hereby recommend that the dissertation be prepared under our supervision by **Deepak Kumar** and Registration number: **00000362796**. Titled: **Wind Turbine Blade Section Optimization Shape Using Improved Genetic Algorithm by Coupling Parameterization** be accepted in partial fulfillment of the requirements for the award of **MS Energy Systems Engineering** degree with (A) grade.

Examination Committee Members

1. Name __Dr. Qazi Shahzad Ali__   Signature: _____

2. Name __Dr. S. A. A. Kazmi__   Signature: _____

3. Name __Dr. Ammar Mushtaq__   Signature: _____

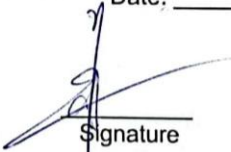Supervisor's name: __Dr. Majid Ali__   Signature: _____

Co-supervisor's name: __Dr. Sehar Shakir__   Signature: _____

Date: __19/12/2024__

Dr. Naseem Iqbal
Head of Department

Signature

20-12-2024
Date

COUNTERSIGNED
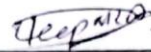
Date: __20/12/2024__

Dr. Adeel Waqas
Dean/Principal

US-Pakistan Center for Advanced Studies in Energy (USPCASE)

CERTIFICATE OF APPROVAL

This is to certify that the research work presented in this thesis, entitled "Wind Turbine Blade Section Optimization Shape Using Improved Genetic Algorithm by Coupling Parameterization" was conducted by Mr. Deepak Kumar under the supervision of Dr. Majid Ali.

No part of this thesis has been submitted anywhere else for any other degree. This thesis is submitted to the Department of Energy Systems Engineering in partial fulfillment of the requirements for the degree of Master of Science. Department of Energy Systems Engineering USPCASE, National University of Sciences and Technology, Islamabad.

Student Name: _____Deepak Kumar_____   Signature: _____

Examination Committee:

    a) GEC Member 1: Dr. Qazi Shahzad Ali   Signature: _____
    (Assistant Professor, USPCAS-E NUST)

    b) GEC Member 2: Dr. S. A. A. Kazmi   Signature: _____
    (Associate Professor, USPCAS-E NUST)

    c) GEC Member 2: Dr. Ammar Mushtaq   Signature: _____
    (Associate Professor, SINES NUST)

Supervisor Name: Dr. Majid Ali   Signature: _____

Co-Supervisor Name: Dr. Sehar Shakir   Signature: _____

Name of HOD: Dr. Naseem Iqbal   Signature: _____

Name of Principal/Dean: Dr. Adeel Waqas   Signature: _____

AUTHOR'S DECLARATION

I, Deepak Kumar, hereby state that my MS thesis titled "Wind Turbine Blade Section Optimization Shape Using Improved Genetic Algorithm by Coupling Parameterization" is my work and has not been submitted previously by me for taking any degree from the National University of Sciences and Technology, Islamabad or anywhere else in the country/ world.

At any time if my statement is found to be incorrect even after I graduate, the university has the right to withdraw my MS degree.

Name of Student:____Deepak Kumar_____

Date: _____ *18-12-24* _____

PLAGIARISM UNDERTAKING

I solemnly declare that the research work presented in the thesis titled "Wind Turbine Blade Section Optimization Shape Using Improved Genetic Algorithm by Coupling Parameterization" is solely my research work with no significant contribution from any other person. Small contribution/ help wherever taken has been duly acknowledged and that complete thesis has been written by me.

I understand the zero-tolerance policy of the HEC and the National University of Sciences and Technology (NUST), Islamabad towards plagiarism. Therefore, I as an author of the above-titled thesis declare that no portion of my thesis has been plagiarized and any material used as reference is properly referred/cited.

I undertake that if I am found guilty of any formal plagiarism in the above-titled thesis even after the award of MS degree, the University reserves the right to withdraw/revoke my MS degree and that HEC and NUST, Islamabad have the right to publish my name on the HEC/University website on which names of students are placed who submitted plagiarized thesis.

Student Signature: _____

Name: _____ Deepak Kumar _____

DEDICATION

This thesis is dedicated first and foremost to my beloved **Parents** for their love, support, and affection. This achievement is as much yours as it is mine. Thank you all for being my pillars of strength.

ACKNOWLEDGMENTS

TABLE OF CONTENTS

LIST OF FIGURES

LIST OF TABLES

LIST OF ABBREVIATIONS, ACRONYMS, AND SYMBOLS

Nomenclature

GA	Genetic Algorithm
ASO	Airfoil Shape Optimization
BC	Boundary Condition
CFD	Computational Fluid Dynamics
AOA	Angle of Attack
HAWT	Horizontal Axis Wind Turbine
VAWT	Vertical Axis Wind Turbine
NACA	National Advisory Committee for Aeronautics
NREL	National Renewable Energy Laboratory
RANS	Reynolds-Averaged Navier–Stokes
SST	Shear Stress Transport
OSU	Ohio State University

Symbols

C	Chord length [m]
$2D$	Two- dimensional
C_L	Co-efficient of lift
C_p	Pressure Co-efficient
C_D	Co-efficient of drag
P_m	Mutation Probability
P_c	Crossover percentage
N	Number of population size
L	Length of string
R_e	Reynolds number
L/D	Lift-to-drag ratio
T	Maximum Thickness [m]

Greek Letters

α°	Angle of attack [degree]
ρ	Air density [kg/m^3]
ε	Epsilon
ω	Omega

ABSTRACT

Airfoil shape optimization is one of the challenging tasks in the designing process of wind turbine blades. The tip airfoil plays a key role in the blade it affects the overall efficiency of the wind turbine, including aerodynamic properties such as coefficient of lift, coefficient of drag, and moment force. In this research endeavor, an improved evolutionary algorithm (genetic algorithm) was explored to optimize the aerodynamic performance of the tip airfoil. A genetic algorithm was coupled with the PARSEC parameterization method to generate the 12 design variables using the sixth degree of polynomial equations. Notable cambered airfoil NREL S810 was incorporated for the aerodynamic analysis and optimization in this study. For the analysis of airfoils, an interactive program of XFOIL was integrated with MATLAB to evaluate the fitness values under the defined geometry constraint of each iterative shape of an airfoil. The results showed that the optimized NREL S810 airfoil exhibited a higher lift coefficient and lift-to-drag ratio compared to the baseline airfoil. Furthermore, the re-verification of genetic algorithm optimized airfoil results was accomplished using the combining Reynolds-averaged Navier Stokes (RANS) with two models $k - \omega$ and $k - \varepsilon$ SST turbulence model. The concluded computational fluid dynamics (CFD) result showed a significant improvement in the coefficient of lift and lift-to-drag ratio of 34.8 % and 19.4 % respectively, at an angle of attack 6.1°, wind speed 14.6 m/s and $R_e = 1$ million compared with experimental data published by the Ohio University State (OUS). Overall, the applicability of design solutions tends to optimize airfoils in less computational time compared to those of traditional ones.

Keywords: Genetic algorithm; airfoil shape optimization; computational fluid dynamics; wind turbine; renewable energy

CHAPTER 1: INTRODUCTION

1.1 BACKGROUND

The need for continuous, reliable, and clean energy is one of the ultimate challenges in the modern world. Presently most of the world's energy requirement is being fulfilled by resources utilizing crude oil (fossil fuels). The energy production using these fossil fuels is costly and CO_2 emissions associated with these fuels are causing environmental concerns. On the other hand, the usage of these fuels at such a large scale has increased the depletion rate of resources of these fuels. Annual production of fossil fuels has been continuously decreasing for the last decade. Therefore, the falloff of greenhouse gas emissions and the replacement of fossil fuel-based energy sources with sustainable and renewable energy sources have been need of hour. The need for a sustainable and efficient source of renewable energy is highly in demand, especially for developing countries. As these renewable energy resources are everywhere to be utilized, therefore, recent years have seen more interest in developing these resources. There are several renewable energy resources that can be exploited, such as solar, wind, geothermal, hydro, biomass, and tidal. Among these renewable energy resources, wind energy can be termed the cleanest, most reliable, and most cost-effective resource. Wind energy is often compared to solar energy. But one of the interesting features of wind energy compared to solar energy is its availability during all times of the day. Therefore, wind energy shows enormous potential as a sustainable solution. Moreover, its production has grown tremendously in recent years. Every new record of installation is achieved, in 2023 a share of 349 GW of solar capacity and 113 GW of new wind capacity was installed.

China is among the top countries that have installed 217 GW and 76 GW of solar after wind respectively and have 60% of renewable scenarios. Therefore, these international trends show a glimpse of a brighter future for wind energy[1]. The below figure highlights the world trend of electricity production share of 7.5% wind 5.1% solar and 87.4% others.
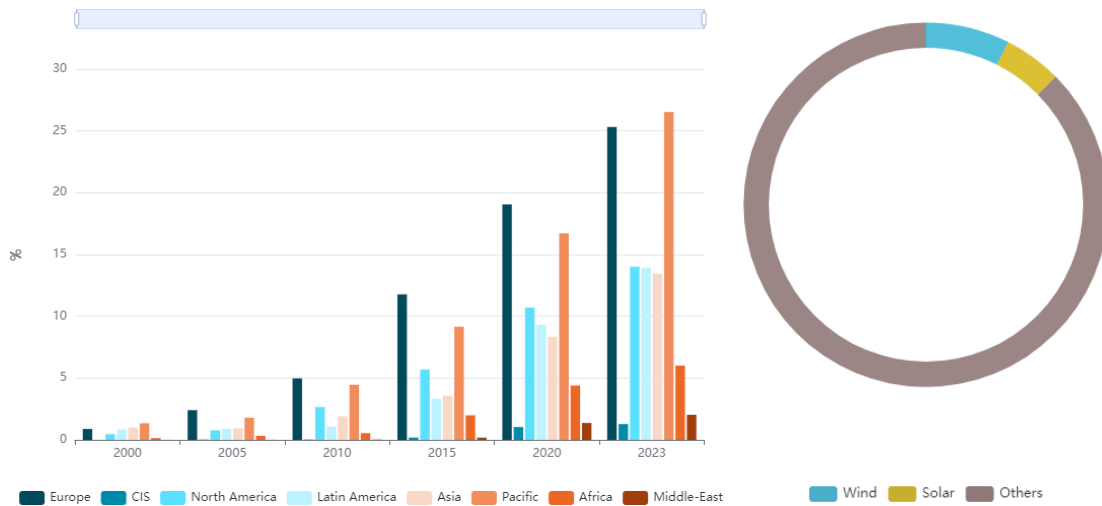
Figure 1-1: The share of Wind energy in the energy mix scenario [1].

The wind is the result of fluctuation in the atmospheric pressure. When there is a difference in atmospheric pressure, air will move from the higher to the lower pressure area, thus resulting in winds of various speeds. Moreover, the wind is tons of air moving around the earth's surface in different directions. For the first time, the wind was used by sailboats to explore other areas of the world. Later on, windmills were invented to extract energy from the wind and use it for pumping water and smashing wheat.

1.1.1   *Classification of Wind Turbine*

A wind turbine is a machine that is used for electricity generation using wind as a source of energy. The working principle of these turbines convert the potential of wind into a useful form of energy using the fundamentals of science and engineering, the impact of incoming wind hits to blade, and rotation is induced due to a force reaction. . The rotor in turn is attached to some gearing system that is coupled with an electrical energy generator. Some wind turbine that operates in closed circuits, for low power requirements, might use a DC generator coupled directly to the rotor. This machine is further divided into two main categories based on application.

a) Horizontal Axis wind turbine and, b) vertical axis wind turbine as shown in figure 2. Much of the work is done on vertical axis wind turbines (VAWT) but due to lower efficiency, the vertical structure increases the wear and tear, limited scalability narrows the window of application, and slow development. Horizontal-axis wind turbines have been the focus of research for many scientists.

2

Figure 1-2: Left side, Horizontal axis turbine, Right side, Vertical axis turbine.

Small-scale wind turbines are being developed (rated power outputs <50 kW) for decentralized power generation. For small-scale applications, HAWT offers a practical option due to its easy operation and easy installation and maintenance. A comprehensive review on the HAWT technology has been presented in ref.[2]. The strong blade-wake interactions and the dynamic vortex shedding together with the vibrations caused by these aerodynamic factors increase the complexity of the VAWT design for aerodynamic and structural designers.

In this regard, different methods to enhance the HAWT rotor aerodynamic characteristics have been highlighted in ref. [3]. Studies have also shown that a number of HAWTs when operated in close proximity can aerodynamically supplement each other resulting in a superior synergic performance and power density. HAWT has resulted in generating more power (between 50 and 100% of power augmentation) compared to a lonely VAWT by taking the assistance of the beneficial induced velocity field[4]. Such an arrangement of multiple wind turbines would be advantageous for a limited area urban population.

Momentum models are extensively applied in the aerodynamic calculation of HAWTs. Moreover, there are three momentum models used, although all are based on the same principle, i.e. to calculate flow velocities passing through a turbine by calculating the streamwise aerodynamic force on the blades, with the variation in the rate of air momentum based on momentum models [5], [6]. The small horizontal axis wind turbine is suitable for low wind speed corridors where wind speed is not more than 5-7 m /s.
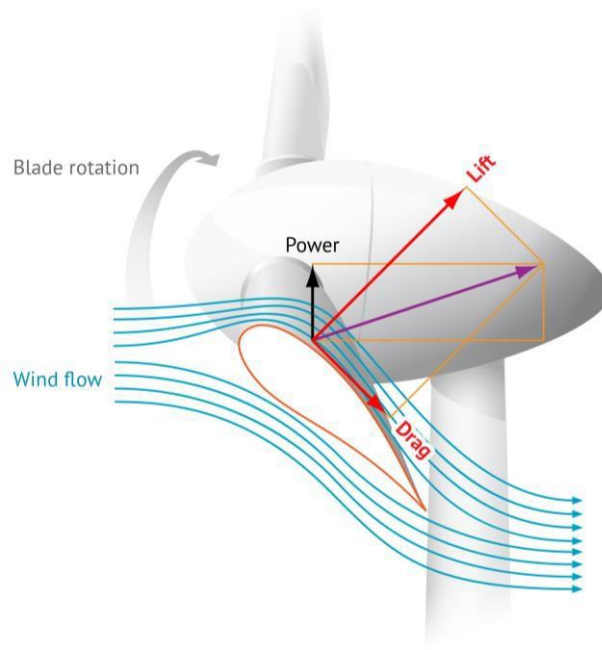
Figure 1-3: Section view of wind turbine blade

1.2 Problem Statement

Horizontal-Axis Wind Turbines (HAWTs) are widely used for renewable energy generation due to their higher efficiency and scalability. However, for small-scale HAWTs (e.g., for residential or urban applications), optimization challenges arise due to fluctuating wind conditions, limited installation space, and the need for cost-effective solutions. Small HAWTs typically suffer from lower power output compared to their larger counterparts, especially in low-wind-speed environments. Moreover, the efficiency of the turbine's blade design, generator performance, and aerodynamic losses significantly impact the overall energy capture.

Current designs often prioritize large-scale applications, neglecting the unique challenges of smaller turbines. These include factors such as blade length, rotor speed, tower height, and yaw control, which need careful calibration to maximize energy efficiency in constrained environments. Additionally, noise reduction and ease of maintenance are critical concerns for small turbines located near residential areas.

The research seeks to explore the optimization of blade geometry, material selection, and turbine control systems to improve the performance of small HAWTs in low-to-moderate wind speeds. The objective is to optimize the small HAWT blade section to enhance the

4

aerodynamic properties, help in the designing process of the wind turbine blade and sustain in wind conditions and suitable for deployment in urban or suburban areas.

1.3 Research Objectives

The oriented goal of this study is to enhance the aerodynamic property of the asymmetric airfoil S-810 using the integrated approach PARSEC parameterization and an improved genetic algorithm for the optimization process.

The research objectives are divided as follows:

- To develop an integrated framework for the optimization using PARASEC parameterization and improved genetic algorithm.

- To optimize the coefficient of lift and lift-to-drag ratio, NREL S-810 airfoil.

- Comparative analysis of the optimized result with baseline experimental data published.

1.4 Scope of Research

The scope of this research involves enhancing the aerodynamic properties of the airfoil S-810 using the improved genetic algorithm. In the design process of wind turbine blades, the airfoil plays a key component in producing the lift force to harvest the electricity from the wind energy. The aim of this study is to improve the aerodynamic property of the horizontal wind turbine blade component which plays a major role in off-design conditions. The scope of this research is not limited to optimizing the airfoil it can be extended to design an optimized blade.

1.5 Limitations

The limitation of this study is that a single optimization technique focused on an improved genetic algorithm for the small horizontal axis wind turbine blade component only. The experimental validation of the optimized airfoil has not been performed. This study is heavily based on simulation which could lead to differences in real-world application.

1.6 Thesis organization

This thesis is structured as follows:

Chapter 1 introduces the background of the topic, and problem statement, and sets the subject of the thesis, delimiting research objectives, limitations, and thesis organization.

Chapter 2 provides a literature review on the green hydrogen role in energy transition with national and international perspectives. It also explains why there is a need to produce green hydrogen in Pakistan.

Chapter 3 presents the selection of an airfoil and the optimization framework of the proposed research methodology and technique used to carry out this research work.

Chapter 4 provides the comparative analysis of computation fluid dynamic (CFD) result of steady state simulation of both airfoils optimized and baseline S810.

Chapter 5 summarizes the research work in the conclusion section and provides future directions for the expansion of this study.

Summary

This chapter introduces the small-scale horizontal axis find turbine blade section's role in the aerodynamic context and its importance and background to the research topic under study with a focus on the problem statement. It also describes the main objectives and research questions along with the scope of this research work followed by thesis organization. Limitations and assumptions have been discussed in this chapter.

CHAPTER 2: LITERATURE REVIEW

2.1 Aerodynamics of Wind Turbine Wing Section

Aerofoil is a 2D shape of a wing, propeller or blade. The wind turbine blade consists of different aerofoils from root to tip each aerofoil has different properties. Air foil shape plays key role in maximizing the overall efficiency of the turbine. The curvature and thickness of the aerofoil determine the how turbine harness the wind at different speed. A well-designed aerofoil balances the aerodynamic parameter including lift and drag force which helps the turbine to capture the maximum energy while minimize the resistance. During the manufacturing of the wind turbine blade multiple parameter are under consideration including the weight of the material, shape of the aerofoil and off design wind condition. Using the advanced computational method close to real time case scenario testing performed to ensure the durability and performance[7]. The below figure 2-1 shows the blade segment with different aerofoil and testing of deflecting flexibility. The aerodynamic forces of lift and drag acting on an airfoil come as a result of the acceleration and deceleration of the flow over the surface of the airfoil.
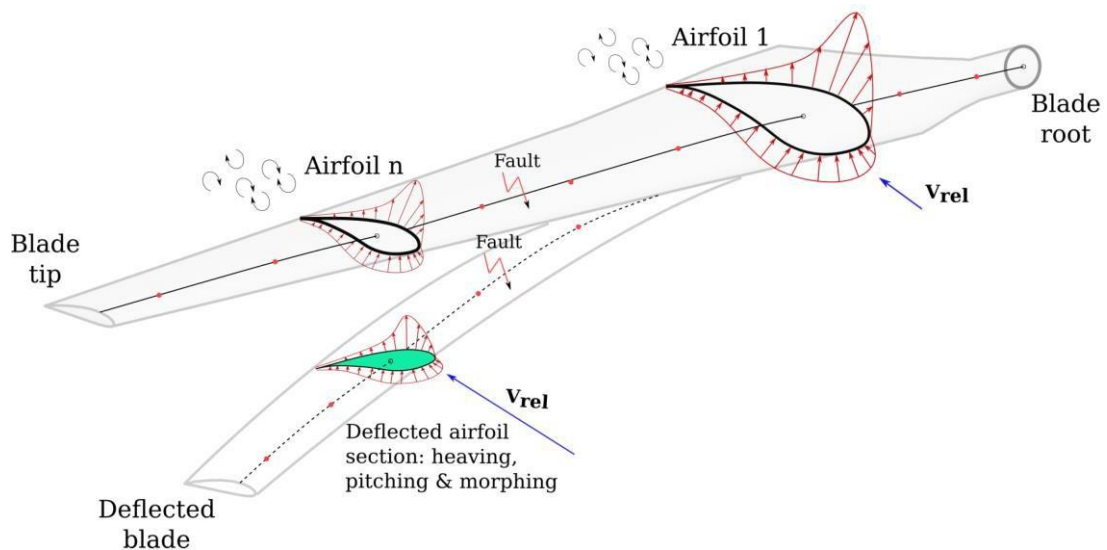
Figure 2-1: Blade design with multiple aerofoil[7].

Which in turn results in pressure forces acting normally on the outer surface of the airfoil. As the fluid molecules are forced around the contour of the airfoil, their velocity and pressure change in accordance with Bernoulli's equation (assuming steady, inviscid, incompressible flow). The higher pressure is exerted on the upper curvature of the airfoil and the lower surface exerts the higher pressure, the difference in these pressures causes the generation of lift force, and the drag force always acts perpendicular to the lift force.
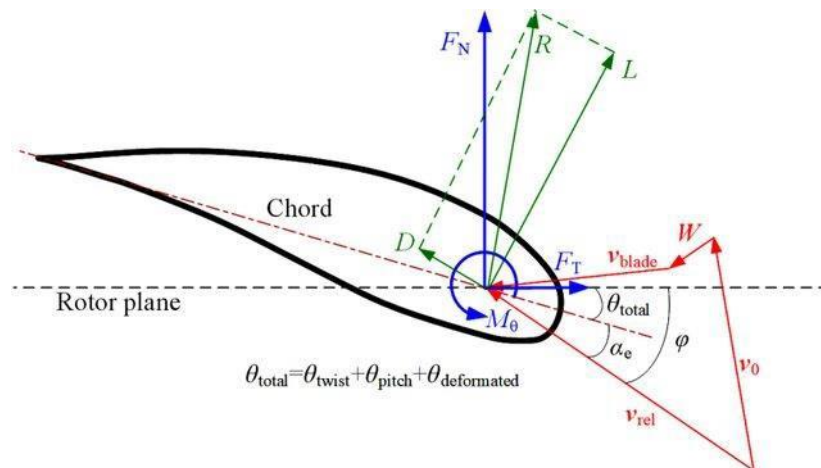
Figure 2-2 Airfoil force velocity triangle[8].

Figure 2-2 briefly describes the velocity triangle of the acting forces on an airfoil and the direction of the moment shows the rotation of the wind turbine blade[8], the key parameter of all force is the angle of attack that describes the strike position of incoming relative wind speed relative to chord length of the airfoil.

Figure 2-3 represents the nomenclature of the aerofoil shape, it consists of two curve upper and lower curves, commonly referred to as the suction and pressure surfaces, respectively. The distance from the leading edge to the tailing edge of the aerofoil is known as chord length[9][2]. The maximum thickness defines the distance between the suction and pressure surfaces, it also helps to determine the position of the aerofoil during the blade design process and generally denoted by the t. The identification of the aerofoil, either it is symmetrical or asymmetrical defined by camber line, or mean line.
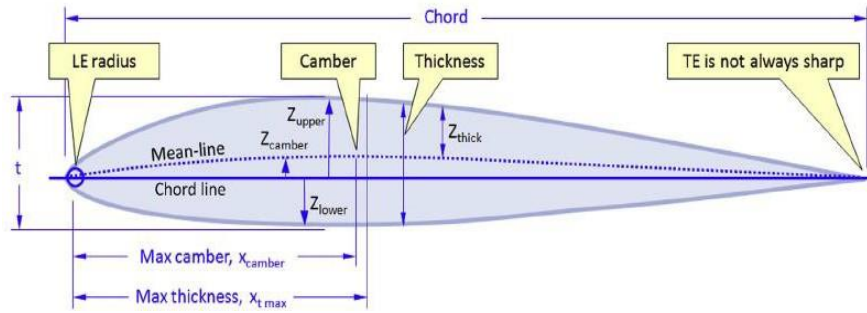
Figure 2-3: Nomenclature of airfoil.

In the blade design process, the size of the blade wind turbine is defined by the maximum thickness, the airfoil family is divided into categories, generally thick airfoil family is used for the large-scale horizontal axis wind turbine, and thin airfoils are considered for the small-scale horizontal axis wind turbine[10], [11]. Figure 2-4 shows both airfoils.
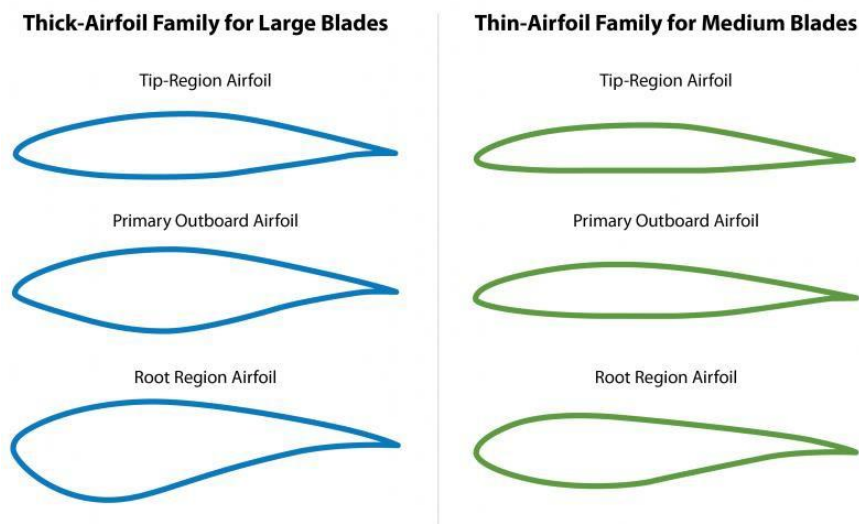
Figure 2-4: Airfoil families.

In a turbine blade the root airfoil is preferable to be thick to provide the structural support of the whole blade and the amount of contribution in the lift generation is much less due to high drag, the middle section airfoil is considered primary outboard, it has dual functionality to create the durability with flexibility in the blade and also contributes the good amount of lift as compared to the root airfoil[12], [13]. The critical part of the blade is the tip airfoil, which generates high lift with low drag, the moment helps to rotate the wind turbine, to maximize the power harness from the wind, and a thin airfoil is preferable for that process.

2.2 PARAMETERIZATION

The parameterization method is a mathematical approach used in optimization and modeling to simplify complex systems by expressing variables or shapes in terms of a set of parameters. parameterization helps define key characteristics like shape, size, or performance metrics using a limited number of variables. By adjusting these parameters, researchers can explore a wide range of design configurations without recreating the entire model[14]. For instance, in wind turbine blade optimization, parameters might include blade length, airfoil curvature, or angle of attack. This method allows for more efficient simulations and sensitivity analyses, as it reduces the dimensionality of the problem while retaining its core physical characteristics. Parameterization also facilitates automatic optimization, where algorithms adjust parameters iteratively to find the best design. In research, this method is crucial for streamlining the design process and improving computational efficiency.

2.2.1. Bezier Curve

A Bezier curve is a parametric curve used in design and modeling to create smooth, flexible shapes. In airfoil shape optimization airfoil's surface can be defined by a few key control points, allowing designers to adjust the leading edge, camber, and trailing edge with ease. These control points act like flexible handles, enabling smooth modifications that impact the aerodynamic performance. By fine-tuning the Bezier curve, engineers can create a wide range of airfoil geometries that adapt to different flow conditions, optimizing for efficiency, stability, and energy capture. The problem of the Bezier curve generates an arbitrary shape due to a less controllable point with an unknown location[15].

$$B(t) = \sum_{i=0}^{6} \left(\frac{n}{i}\right)(1-t)^{n-i} t^i P_i \tag{1}$$

2.2.2. Class Shape Transformation (CST)

The Class-Shape Transformation (CST) method is a flexible and robust parameterization technique used primarily in airfoil and aerodynamic shape optimization. It separates the airfoil or wing shape into two distinct components:

a)   The Class function defines the general geometric characteristics of the airfoil, including the leading edge, trailing edge, and overall aerodynamic characteristics.

$$C(x) = x^N(1-x)^M \qquad (2)$$

b)   The Shape function modifies the specific contour of the airfoil by controlling its thickness, camber, and curvature at various points along the chord. This function is often represented as a polynomial or a set of coefficients.

$$S(x) = \sum_{i=0}^{n} x\, a_i \qquad (3)$$

The final equation after combining both equations 1 and 2 for the airfoil optimization.

$$y(x) = C(x).S(x) \qquad (4)$$

Class Shape Transformation (CST) is more flexible with fewer control points make less reliable for airfoil optimization. However, to overcome the curve fitting and search space gap a well-known parameterization method is PARSEC[16].

2.2.3.   PARSEC

The precision of the control points helps to predict better aerodynamic results. The PARASEC parameterization provides the 12 design variables that divide the airfoil shape into two halves upper surface and lower surface from the leading edge to the tailing edge. The sixth degree of polynomial makes the curve fit better over the surface of the airfoil[17], [18].

For the upper curve of the airfoil, the equation will be.

$$y_u = \sum_{i=1}^{6} a^i{}_{up} x^{i-(0.5)} \qquad (5)$$

For the lower curve of the airfoil, the equation will be.

$$y_l = \sum_{i=1}^{6} a^i{}_{up} x^{i-(0.5)} \qquad (6)$$

11

2.3 Optimization Schemes

Over the decade optimization techniques have been changing to achieve the ideal shape of airfoils from numerical methods to a number of datasets. Blade element theory (BEM) numerical-based approach by changes the fundamental parameters including the twist and chord angle of the blade section instead of the airfoil shape. Adjoint-based airfoil optimization used coupling with B-spline parameterization results were insignificant for future work[19]. Zhang et al.[20] and Li et al.[21] Summarizes the challenge of machine learning is that prediction models often require large datasets and complex tuning. Which is not feasible for small horizontal-axis wind turbine airfoils at certain flow conditions. Unlike machine learning models, which act as black boxes.

Genetic algorithms provide a better understanding of influencing performance variables[22]evidence after the performance analysis of multiple meta-heuristic algorithms. The genetic algorithm shows significant convergent results in less time to optimize the airfoil. Asymmetric airfoil NACA 9415 aerodynamically optimized in novel technology airborne wind turbine using the PARSEC parameterization and genetic algorithm [23], [24], [25], [26]. However, there is a window to improve the operator of a genetic algorithm.

2.4 Computational Fluid Dynamics (CFD)

In the engineering domain, computational studies serve as a key tool for performing real-time analysis and understanding the behavior of complex systems. This approach is particularly important in the optimization of airfoils. Where advanced parameterization techniques are required. An airfoil parameterization method was combined with an orthogonal algorithm, and computational fluid dynamic (CFD) predictions were integrated to fulfill the objective [27]. This study [28] performed computational fluid dynamics after the optimization using the S-A turbulence model which shows a good agreement with the initial result with an error of 1.41%. Our research group [29],[30], [31] evaluates the fitness function via grid Navier–Stokes flow solver with a two-equation $K-\varepsilon$ turbulence model. Standalone CFD optimization is not enough to make the design better [2] coupling CFD analysis with advanced algorithms helps to overcome the challenges of multidisciplinary analysis and optimization. However, the previous studies show that combining both approaches parameterization and CFD optimization has not covered a gap in aerodynamic properties

improvement and overall small horizontal axis wind turbine (HAWT) performances. Therefore, the creation of a technical and more systematic approach is evaluated by combining the multiple approaches as described in the next section.

Summary

This chapter provides an overview of existing studies conducted on airfoil shape optimization using multiple Parameterization techniques coupled with multiple algorithms to enhance the aerodynamic properties of the airfoil. Using the computational fluid dynamics simulation, the behavior of the optimized airfoil predicts various wind conditions with different angles of attack to ensure the off-design flexibility for small-scale horizontal axis wind turbines.

CHAPTER 3: METHODOLOGY

3.1 PARSEC Parameterization

A well-known parameterization technique, PARSEC was used to create the initial design variable of the subsonic and transonic airfoils, a method developed by Sobieczky [32]. The key concept of this method is to generate six design variables from multiple points of individual airfoil surfaces both upper and lower. The design variable of each curve surface is defined by a sixth-degree polynomial in Equations (7) and (8) respectively.

$$y_u = \sum_{i=1}^{6} a^i_{up} x^{i-(0.5)} \tag{7}$$

$$y_l = \sum_{i=1}^{6} a^i_{lo} x^{i-(0.5)} \tag{8}$$

Where y_u and y_l express the y-ordinates of the upper and lower surface curves respectively, a^i_{up} and a^i_{lo} are the unknown coefficients of upper and lower curvature, x represents the cord-wise distance. The unknown coefficient can be determined by solving the 12 linear algebraic equations simultaneously as given by:

$$C_{upper} * a_{upper} = b_{upper} \tag{9}$$

$$C_{lower} * a_{lower} = b_{lower} \tag{10}$$

Where,

$$
C_{upper} =
\begin{bmatrix}
1 & 1 & 1 & 1 & 1 & 1 \\
p_3^{1/2} & p_3^{1/2} & p_3^{1/2} & p_3^{1/2} & p_3^{1/2} & p_3^{1/2} \\
\dfrac{1}{2} & \dfrac{3}{2} & \dfrac{5}{2} & \dfrac{7}{2} & \dfrac{9}{2} & \dfrac{11}{2} \\
\dfrac{1}{2}p_3^{-1/2} & \dfrac{3}{2}p_3^{1/2} & \dfrac{5}{2}p_3^{3/2} & \dfrac{7}{2}p_3^{5/2} & \dfrac{9}{2}p_3^{7/2} & \dfrac{11}{2}p_3^{9/2} \\
-\dfrac{1}{4}p_3^{-3/2} & \dfrac{3}{4}p_3^{-1/2} & \dfrac{15}{4}p_3^{1/2} & \dfrac{35}{4}p_3^{3/2} & \dfrac{63}{4}p_3^{5/2} & \dfrac{99}{4}p_3^{7/2} \\
1 & 0 & 0 & 0 & 0 & 0
\end{bmatrix}
\tag{11}
$$

$$
C_{lower} =
\begin{bmatrix}
1 & 1 & 1 & 1 & 1 & 1 \\
p_6^{1/2} & p_6^{1/2} & p_6^{1/2} & p_6^{1/2} & p_6^{1/2} & p_6^{1/2} \\
\dfrac{1}{2} & \dfrac{3}{2} & \dfrac{5}{2} & \dfrac{7}{2} & \dfrac{9}{2} & \dfrac{11}{2} \\
\dfrac{1}{2}p_6^{-1/2} & \dfrac{3}{2}p_6^{1/2} & \dfrac{5}{2}p_6^{3/2} & \dfrac{7}{2}p_6^{5/2} & \dfrac{9}{2}p_6^{7/2} & \dfrac{11}{2}p_6^{9/2} \\
-\dfrac{1}{4}p_6^{-3/2} & \dfrac{3}{4}p_6^{-1/2} & \dfrac{15}{4}p_6^{1/2} & \dfrac{35}{4}p_6^{3/2} & \dfrac{63}{4}p_6^{5/2} & \dfrac{99}{4}p_6^{7/2} \\
1 & 0 & 0 & 0 & 0 & 0
\end{bmatrix}
\tag{12}
$$

$$
b_{upper} =
\begin{bmatrix}
\left(\dfrac{p_9+p_{10}}{2}\right) \\
p_4 \\
\tan\left(\dfrac{p_{11}-p_{12}}{2}\right) \\
0 \\
p_5 \\
\sqrt{2p_1}
\end{bmatrix}
\tag{13}
$$

$$
b_{lower} =
\begin{bmatrix}
\left(\dfrac{p_9-p_{10}}{2}\right) \\
p_7 \\
\tan\left(\dfrac{p_{11}+p_{12}}{2}\right) \\
0 \\
p_8 \\
\sqrt{2p_2}
\end{bmatrix}
\tag{14}
$$

These 12 design variables define the airfoil shape with a unit chord length and directly control the airfoil aerodynamics such as leading-edge radius, maximum thickness, and tailing edge wedge angle enlisted in Table 3-1.

Table 3-1: Description of 12 PARSEC parameters

PARSEC parameters	Shape parameter	Definition
p_1	r_{leup}	Upper leading-edge radius
p_2	r_{lelo}	Lower leading-edge radius
p_3	X_{up}	Upper crest position in horizontal coordinates
p_4	y_{up}	Upper crest position in vertical coordinates
p_5	y_{xxup}	Upper crest curvature
p_6	X_{lo}	Lower crest position in horizontal coordinates
p_7	y_{lo}	Lower crest position in vertical coordinates
p_8	y_{xxlo}	Lower crest curvature
p_9	y_{te}	Trailing edge offset in a vertical sense
p_{10}	Δy_{te}	Trailing edge thickness
p_{11}	α_{te}	Trailing edge direction
p_{12}	β_{te}	Trailing edge wedge angle
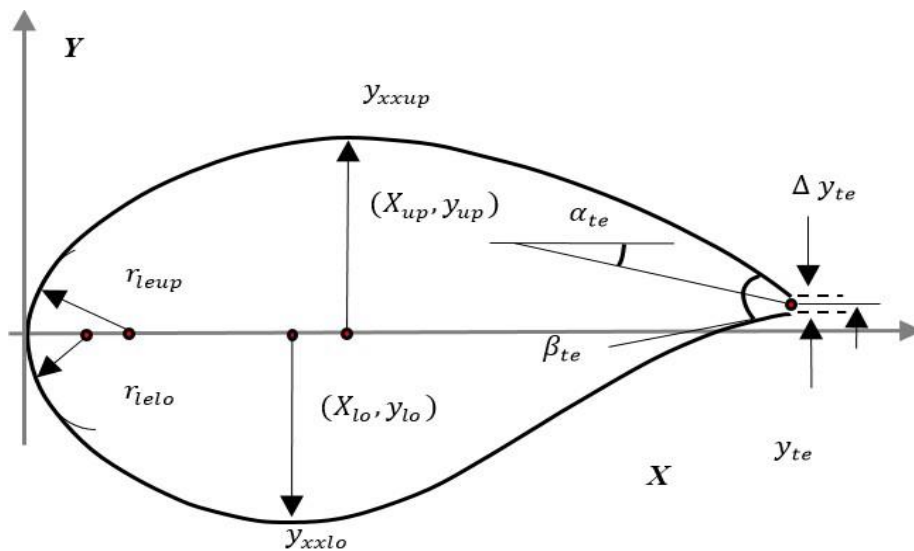
Figure 3-1 PARSEC design variables of an airfoil.

The previous literature shows that different types of parameterization techniques were adopted to transform the shape of the airfoil with a minimum possible number of control points (design variables). The precision of the control points helps to predict better aerodynamic results. The PARSEC parameterization provides the 12 design variables which divided the airfoil shape into two halves upper surface and lower surface from the leading edge to the tailing edge as described in figure 3-1. The square tailing edge makes the structure mesh sophisticated. To simplify the mesh generation process and minimize dynamic stall, the tailing edge of the airfoil was created sharp by keeping the design variables p_9 and p_{10} zero as shown in Table 3-2 [33]. The second column shows the design variable of the base airfoil. The third and fourth columns show the bounds limit of both the upper and lower surface of the design space created using the tolerance $^+10\%$ of the design variables. The fourth column shows the design variable of the optimized using the genetic algorithm. Figure 3-2 shows the curve fitting of the PARSEC parametrization.

Table 3-2: 12 design variables with upper and lower bounds.

Design variables	Base airfoil	Upper bounds	Lower bounds
p_1	0.013	0.011	0.015
p_2	0.004	0.003	0.005
p_3	0.432	0.367	0.497
p_4	0.096	0.081	0.110
p_5	-0.839	-0.714	-0.965
p_6	0.427	0.363	0.492
p_7	-0.085	-0.072	-0.098
p_8	1.188	1.010	1.366
p_9	0.0	0	0
p_{10}	0.0	0	0
p_{11}	-7.048	-6.942	-7.154
p_{12}	3.945	3.886	4.004
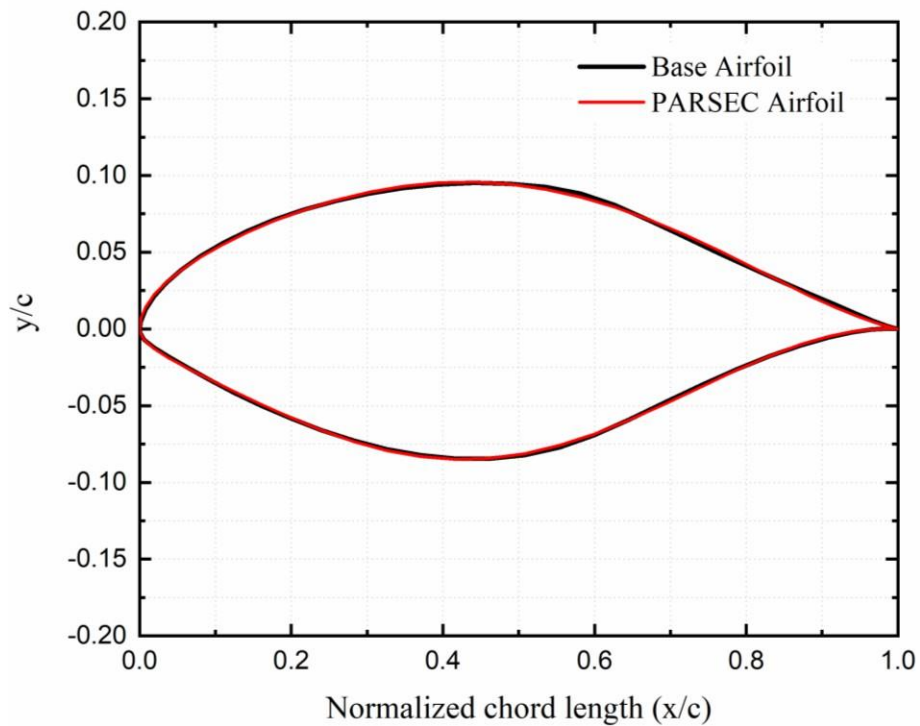
Figure 3-2: Base airfoil and PARSEC parametric airfoil.

3.2 Genetic Algorithm

A heuristic method based on natural search selection is known as the Genetic algorithm. Based on Darwin's principle, of survival of the fittest, John Holland developed this algorithm to design an artificial system to retain the mechanism of the natural system [34]. Genetic algorithms can be used to solve both linear and nonlinear optimization problems. However, they are particularly effective for nonlinear optimization problems. Where, traditional optimization methods struggle due to complexity, non-convexity, or high dimensionality [35]. In the field of aerospace and wind turbine problems are nonlinear, to achieve the global optimum to enhance the overall efficiency of the system via real coded algorithm [36]. The genetic algorithm is an iterative process. Each iteration is called generation, initially a random population generated using a domain of search space with a set of strings, each string consists of a character (for this study 12 design variables). Each string goes for fitness evaluation under the defined criteria of fitness function (maximum thickness and coefficient of lift). Normally the strings are chosen near to fitness value and go for further process of parents' selection, commonly used roulette wheel. The selected pair of parents will go

18

under genetic operators' crossover and mutation. The iteration process goes on until the termination criteria are met [37]. Table 3-3 shows the computation of the genetic algorithm.

Table 3-3: Computation of Genetic Algorithm.

Natural representation	GA representation
Chromosome	String
Gene	Character
Allele	Character's value
Locus	String position

3.2.1.   Search Spaces

Search space is a region to generate the possible airfoil shape under a defined limit with upper and lower bounds of each design variable[37].

$$l_b \leq x \leq u_b \tag{15}$$

Where, l_b is the lower bound and u_b is the upper bound, x represents the design variables.

3.2.2.   Initial Population

The initial population in the genetic algorithm consists of a set of candidate solutions, each represented as a string. These strings are randomly generated within the search spaces typically reflecting possible solutions. Random numbers are generated between 0 and 1. The size of initial population is controlled by population size. It is a crucial part of genetic algorithms [17, 21] to suggest an appropriate population size to gain the computational advantage using an empirical way, given by

$$N = 4l \tag{16}$$

Where N represents the population size and l the length of a string

3.2.3. *Parents Selection*

The selection process begins by choosing random individuals from the pool of the initial population and selecting the best out of these to become parents. The purpose of the parents is to act as mates and recombine to generate offspring. Numerically, the selection process of parents is accomplished through the fitness function. The value of fitness based on geometric constraints is suitable for the fitness evaluation of individual parents[37]. Similarly, each offspring is evaluated in a similar way to pass the fitness criteria. In this study, the thickness of the original airfoil was used as fitness criteria, and the tournament selection technique was used to maintain good diversity and avoid premature convergence[38], [39]. Moreover, various selection techniques are also available for instance Roulette wheel, Stochastic Universal Sampling (SUS), and Rank selection.

3.2.4. *Cross Over*

The crossover operator is the backbone of the search algorithm performed via design space. The information contained in one string (parent_1) and the other selected string (parent_2) combine both to crossover the genes to get a new offspring (child). The string of the resulting offspring only survives if it has a good fitness evaluation and then exchanges the newly acquired string of genes again in the next generation. For optimization, a uniform crossover gives better results unlike the single or multi-point crossover based on experimental results[42] and usually known as crossover percentage P_c.

3.2.5. *Mutation*

The mutation operator is used to flip the bit of the offspring string from 0 to 1 or vice versa. Subsequently, the cross-over, mutation operator is used to avoid local minimum and maintain the genetic diversity in the population. Mutation probability (P_m) is used to describe the percentage of the diversity of the offspring string and empirical guidelines are given by [42].

$$P_m = \frac{l + 1}{2Nl} \tag{17}$$

Where, P_m, l, and N are mutation probability, length of string, and population size respectively. Table 3-4 shows the parameter value considered in the study

Table 3-4: Algorithm Parameters and their values.

Algorithm Parameters	Values
Length of string	12
Population size	48
Crossover percentage	0.75
Mutation probability	0.02

3.3 Objective Function

The objective function is the key concept of the optimization process. It can maximize or minimize the effect of a particular entity to enhance the performance of the system. Choosing suitable objective and constraint functions is essential for any design optimization challenge, for this study table 3-5 is stated.

Table 3-5: Optimization objective and constraint.

Geometrical constraint	p_9 & p_{10} are set to zero.
Aerodynamics constraint	$C_{l\ optimized} > C_{l\ original}$ Angle of Attack $= 0°$ and $6.1°$ Maximum thickness $(0.01 < T_{original} < 0.1)$
Objective	Maximize C_l
Termination criteria	No change in $C_{l\ optimized}$ after the 10 generations

3.4 XFOIL

XFOIL is an interactive program used for analyzing the aerodynamic properties of airfoils. Mostly used in airfoil design optimization and performance analysis, applications for

aircraft, and wind turbines. The numerical algorithm of XFOIL incorporates a panel method for calculating the key parameters, including are coefficient of lift, drag, and moment. The results are based on each number of panels which further provides a cumulative effect based on input geometry and operation conditions.

The proposed methodology is in Figure 3-3. A geometry shape of the airfoil S-810 was created using the data set of coordinates. PARSEC, a numerical parameterization technique was used to generate the 12 design variables using sixth-degree polynomial equations under the MATLAB environment and an improved genetic algorithm code was created. Using an XFOIL script, under the defined geometric and aerodynamic constraint, the evaluation of the fitness function of each newly generated airfoil shape was compared with the original one.
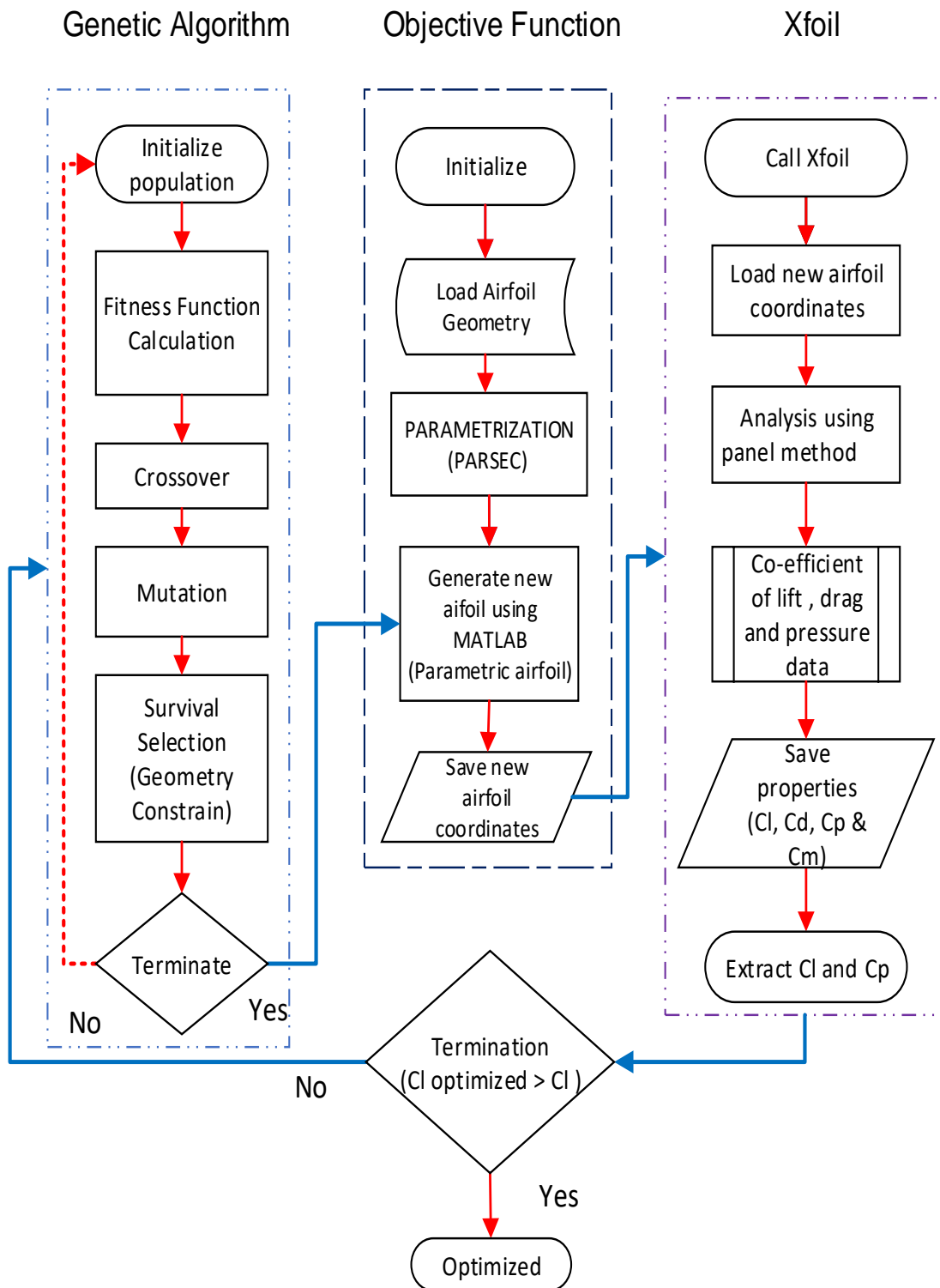
Figure 3-3: Workflow of the optimization process in MATLAB.

After a certain number of function evaluations, the result converged toward the optimization and the final optimized airfoil shape S-810 showed very promising results in terms of high lift coefficient at 0° and 6.1° angle of attack. After that, a computational fluid dynamic simulation study of steady state was performed on both airfoils original and optimized, using the ANSYS FLUENT.

Summary

In this chapter, the PARASEC parameterization method is used to generate the 12 design variables of the airfoil S-810, for the curve fitting. Using an improved genetic algorithm, design variable feed as an initial population of the iterative process, and each iteratively generated shape via multiple genetic operators including parent selection, cross over, and mutation to increase the diversity of the search space. Individual shape undergoes defined objective function and geometry constraints, panel method is used to perform the aerodynamic flow analysis of individual iterative shapes using the XFOIL, a defined script created with flow conditions.

CHAPTER 4: COMPUTATIONAL MODEL

4.1 Computational Fluid Dynamics (CFD)

This section evaluates the in-depth analysis of the 2D airfoils using the Reynolds-averaged Navier-Stokes (RANS) equation for steady state and incompressible flow field study analysis is carried out using the Software ANSYS-Fluent®. Equations represent the tensor form of the mass and momentum, respectively.

$$\frac{\partial u_i}{\partial x_i} = 0 \tag{18}$$

$$\rho u_j \frac{\partial (u_i)}{\partial x_j} = -\frac{\partial p}{\partial x_i} + \mu \frac{\partial^2 u_i}{\partial x_j \partial x_j} + \frac{\partial}{\partial x_j}\left(-\rho \overline{u_i u_j}\right) + \rho f_{b,i} \tag{19}$$

Where density, pressure, dynamic viscosity, and body force are represented by $\rho, p, \mu,$

and f_b respectively. The fluid velocity vector is represented by u_i ($i = 1$) and u_j ($j =$

2) and the Reynolds stress in turbulent flow is represented by $-\rho \overline{u'_i u'_j}$ where u'_i and u'_j

represent the velocity fluctuation in the turbulent flow. To evaluate the accurate prediction of aerodynamic properties shear stress transport (SST) model is adopted. The advantage of this model is to incorporate the effect of a near wall using the $k - \omega$ (k omega) model which helps understand the behavior of the flow near the boundary layer as the flow moves away from the surface in the free stream region transition start and the changing of this behavior is noticeable by $k - \varepsilon$ (k epsilon) model[30]. This transition of the flow depends on the mesh model and mesh quality helps to avoid the pre-convergence which leads to inaccurate prediction.

4.2   Mesh Models

The accuracy of CFD result prediction is relay on the mesh model. A 2D black structured grid domain is created using the C-type topology Fig.3-4 and the domain sizing is mentioned [25], [26], [27]. The domain is further divided into subdomains to analyze the effect of fluid flow transition from the model surface (boundary layer) to the free stream region (far field). To ensure the smooth transition the quality of the mesh is defined by the mesh matrices including aspect ratio, skewness, and orthogonally in Table 4-1. The growth rate is set to default at 1.2 and set the mesh medium from course to fine. The transition ratio and maximum layer are set at 0.272 and 2 respectively.

Table 4-1: Mesh Matric.

Mesh matric parameters	Minimum	Maximum	Standard deviation
Aspect ratio	1	$1.045E^5$	4379.4
Skewness	$1.3057E^{-10}$	0.65072	0.10135
Orthogonal quality	0.002141	1	0.076802

Besides to ensure the meshing quality at the boundary of the airfoil the distance from the wall to the first cell of the boundary should be <1 to be considered. It is a critical parameter when dealing with the turbulence simulation. To better control the simulation result using the SST turbulence model keep the y^+ value less than one by increasing the no of elements and bias factor to take advantage of the C-type domain Figure 4-1. The equation (20) is used to calculate the y^+ value.

$$\Delta y = L y^+ \sqrt{74} \ R_e^{-\frac{13}{14}} \tag{20}$$

Where Δy , L and R_e represent the distance from the wall to the first node, the flow length, and the Reynolds number respectively.
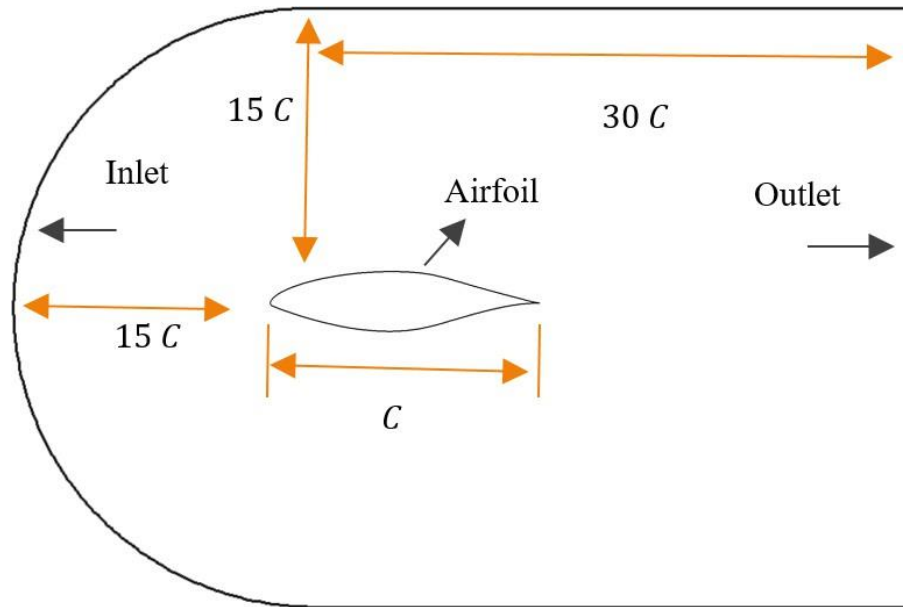
Figure 4-1: The C-type domain of grid meshing.
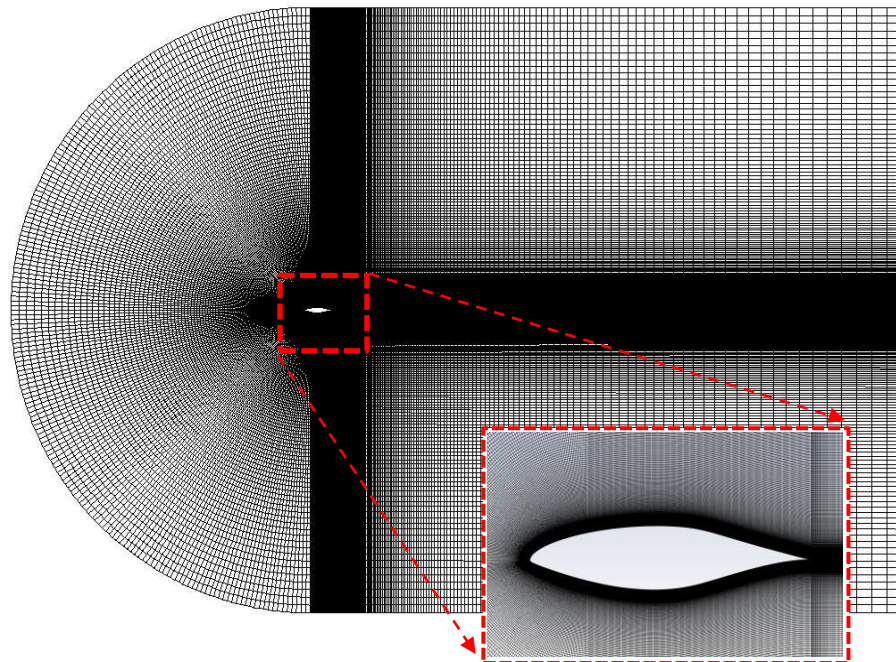
Figure 4-2: Structured mesh grid of base airfoil at $0°$ Angle of attack.

(a)   (b)
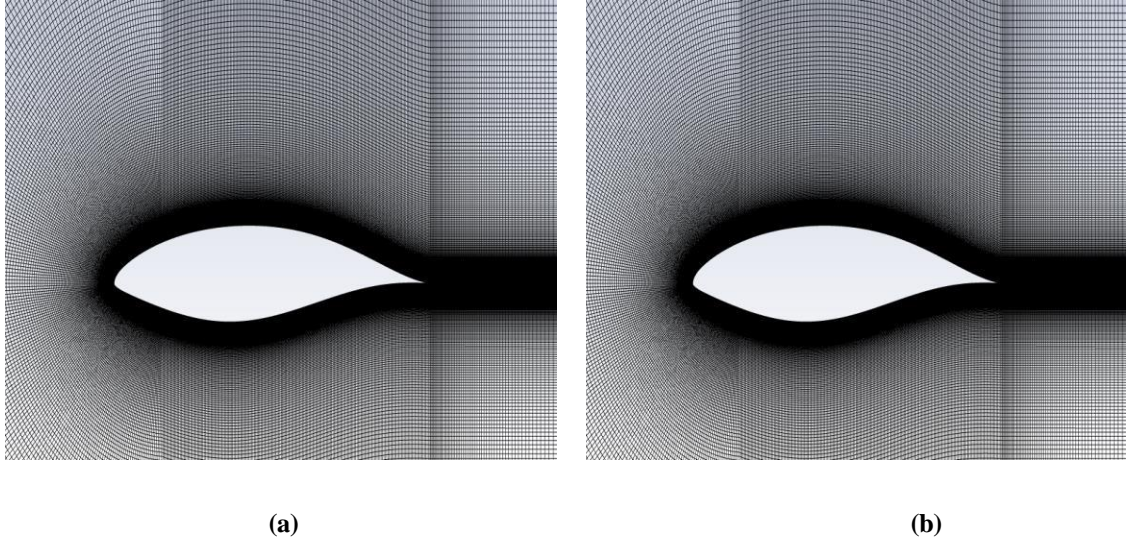
Figure 4-3: (a) The Right side is the base airfoil. (b) The left side is a GA-optimized
airfoil.

4.3   Boundary Conditions (BCs)

`   This section highlights the boundary condition for a 2D structured mesh grid, the
domain's inlet condition was set to an inlet velocity of $14.6 m/s$ defining both components
in V_x and V_y flow direction using the equations (21) and (22) respectively.

$$V_x = V cos(\alpha°) \tag{21}$$

$$V_y = V sin(\alpha°) \tag{22}$$

Where V represents the flow velocity and $\alpha°$ represents the angle of attack in degrees.
For the turbulence, the intensity and viscosity ratio is set to 5% and 1 respectively [44]. For the
domain's outlet, the gauge pressure is set to zero, and turbulent backflow intensity and ratio
are set to 5% and 10 respectively. Consider the airfoil and wall surface as stationary walls
and apply no slip shear condition with the standard roughness model.

4.4   CFD Solver Setup

The ANSYS fluent v.19.3 was used to perform the all simulations of this study. The shear stress transport (SST) model is selected from the viscous model to capture the effect of flow transition at the boundary layer and far-field domain. The reference values were computed from the inlet domain condition and the other parameters including density, pressure, temperature, and viscosity are standard. Under the solution methods, the coupled scheme was selected and set the discretization second order upwind to avoid the early convergence error unable to the pseudo transient option. The relaxation factor is set to 0.5 and defines the report forces coefficient of lift C_l and coefficient of drag C_d under-report definition.

$$C_l = \frac{F_l}{\frac{1}{2}\,\rho\,v^2 A} \tag{23}$$

$$C_d = \frac{F_d}{\frac{1}{2}\,\rho\,v^2 A} \tag{24}$$

$$R_e = \frac{\rho\,v\,L}{\mu} \tag{25}$$

Where F_l , F_d , ρ , v , L , μ , A are the lift force, drag force, density, the velocity of the fluid, characteristic length (chord length), the dynamic viscosity of a fluid, and area respectively. In the residual monitors, the convergence absolute criteria are defined as $1e^{-6}$ and run the 3K iteration after the hybrid initialization.

4.5 Mesh Sensitivity Model

The mesh sensitivity analysis is a strategic component in a computational domain that helps to choose the right meshing element numbers to save computational costs over time. This study was carried out with five different structured mesh models, using the multiple mesh element numbers from 0.1 to 1.6 million. Details are listed in Table 4-2, all the steady-state simulations of the grid (M1-M5) were performed at wind speed 14.6 m/s with an angle of attack of 6.1°. After each independent grid study, the results were compared based on aerodynamic properties (C_L and C_D) and process time of three thousand iterations. An error of less than 1% was seen during the transition of M2 to M3 in the aerodynamic properties of the

airfoil. Therefore, grid M3 was considered for this study over M4 and M5 to avoid the computational cost over time with acceptance of error.

Table 4-2: Grid sensitivity analysis.

Grid	No of element (million)	y^+	C_D	C_L	Average CPU Process time (min)
M1	0.1	0.9	0.0077	0.9139	3.7
M2	0.2	0.75	0.0081	0.9273	18.8
M3	0.4	0.48	0.0082	0.9249	41.7
M4	0.8	0.37	0.0085	0.9218	168.7
M5	1.6	0.27	0.0086	0.9203	1134.3

Summary

This chapter discusses the steady-state simulation of 2D analysis of the optimized and baseline airfoil performed using the ANSYS FLUENT. A black structured grid is created with a suitable domain size and divided into subdomains to analyze the effect of the boundary layer near the wall and far field. Mesh independence analysis was performed to ensure the right number of elements to save the computational cost over time. After the boundary condition the shear stress transport (SST) model was selected to capture both the effect of flow transition at the boundary layer and far-field domain.

CHAPTER 5: RESULTS AND DISCUSSION

This section summarizes the all results that were carried out during the study via integrating the PARSEC parameterization with the improved genetic algorithm optimization technique used to enhance the aerodynamic properties of the NREL S-810 airfoil of horizontal axis wind turbine (HAWT). The wind tunnel data published by the Ohio State University (OSU) [45] is a supported document to compare the optimization results and evidence shows a good agreement of the aerodynamic forces enhancement. The oriented goal of this study is optimization and Computational Fluid Dynamic (CFD) simulation of the airfoil to ensure they maximize the lift-to-drag (L/D) ratio and the coefficient of lift (C_L). For the optimization approach, the parameterization and the genetic algorithm coding were integrated using MATLAB interference. In addition, the panel method technique was adopted to calculate the aerodynamic parameters including were C_L, C_D, and C_p coefficient of lift, drag, and pressure respectively using the XFOIL. The Computational fluid dynamics simulation process was performed using the ANSYS Fluent, a 30 times chord C-type domain was created for the flow field analysis the domain was further divided into subdomains to capture the near wall effect of the flow on the airfoil surface. For that process the mesh element was selected after performing the mesh independence test shown in Table 3-7, The M3 grid was considered based on less the 1% error than M4 and M5 respectively, to save the computational cost over time.

5.1 Model Validation

This section relates to the validation and optimization of the base airfoil NREL S-810 airfoil. Initially, the airfoil was selected with a constant chord length of 0.457m (18 inches) [45]. The chord length was normalized with the x-axis to perform the rest of the analysis. The chord length was normalized with the x-axis to perform the rest of the analysis. The PARSEC parameterization was used to generate the design variables from the coordinate data set to re-create the airfoil shape defined into two halves via upper and lower surface, each surface has six design variables obtained from six degrees of polynomial equations. After that, those design variables were initially fed to the genetic algorithm as a population with search space of each design variable under defined geometry constraint and objective function. To ensure the fitness of the objective function during the optimization process the aerodynamic analysis

was performed with defined flow conditions including. R_e= 1million, angle of attack (AOA) = 0° and 6.1°.

Mach number = 0.042 and the wind velocity of 14.6 m/s. A script file was created with defined flow conditions, via the panel method using XFOIL all the results were extracted and saved to compare each iterated airfoil shape till the objective criteria were achieved. In Table 5-1. The third Column represents the optimized 12 design variables, which are obtained using the improved genetic algorithm code in a house of MATLAB. These design variables were generated after the evaluation of the fitness criteria of each iterated shape of an airfoil. Search space was defined via the upper and lower surface limits of +10% of the base airfoil design variable.

Table 5-1: Optimized 12 PARSEC design variables.

| Design variables	Shape variables	Optimized
p_1	r_{leup}	0.0127
p_2	r_{lelo}	0.0048
p_3	X_{up}	0.4948
p_4	y_{up}	0.1075
p_5	y_{xxup}	-0.8727
p_6	X_{lo}	0.3840
p_7	y_{lo}	-0.0749
p_8	y_{xxlo}	1.3480
p_9	y_{te}	0
p_{10}	Δy_{te}	0
p_{11}	α_{te}	-7.0365
p_{12}	β_{te}	3.9905

Figure 5-1 shows both airfoils optimized and base airfoil, optimized airfoil was generated via 12 design variables and separated into upper and lower curves via 6 design variables.
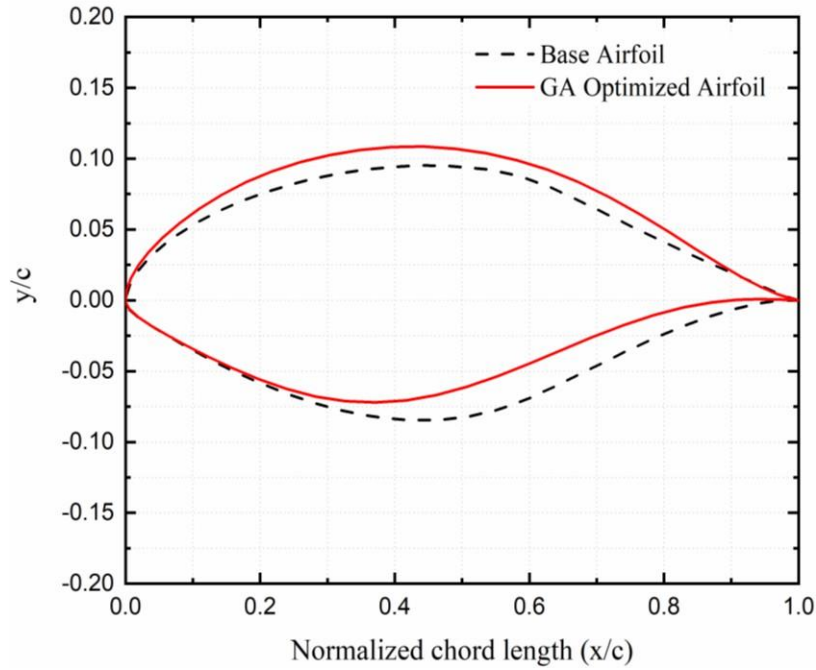
Figure 5-1: Base airfoil and genetic algorithm optimized airfoil.

The lower curve shows the inward trend considering the base airfoil and wise verse for the upper curve, which results in a higher coefficient of lift (C_L) and lift-to-drag ratio(C_L/C_D). Figure 5-2 shows the evaluation of each iterated shape of airfoil generated via genetic algorithm. Figure 5-2 (a) Shows the coefficient of lift (C_L) analysis performed via XFOIL, each airfoil shape in search space at an angle of attack $0°$. Figure 5-2 (b) Shows the coefficient of drag (C_D) and pressure coefficient (C_p) distribution over the surface of each evaluated airfoil. After 800 iterations, there was no change in the coefficient of drag, and the optimized shape of the airfoil was achieved with defined constraint parameters.
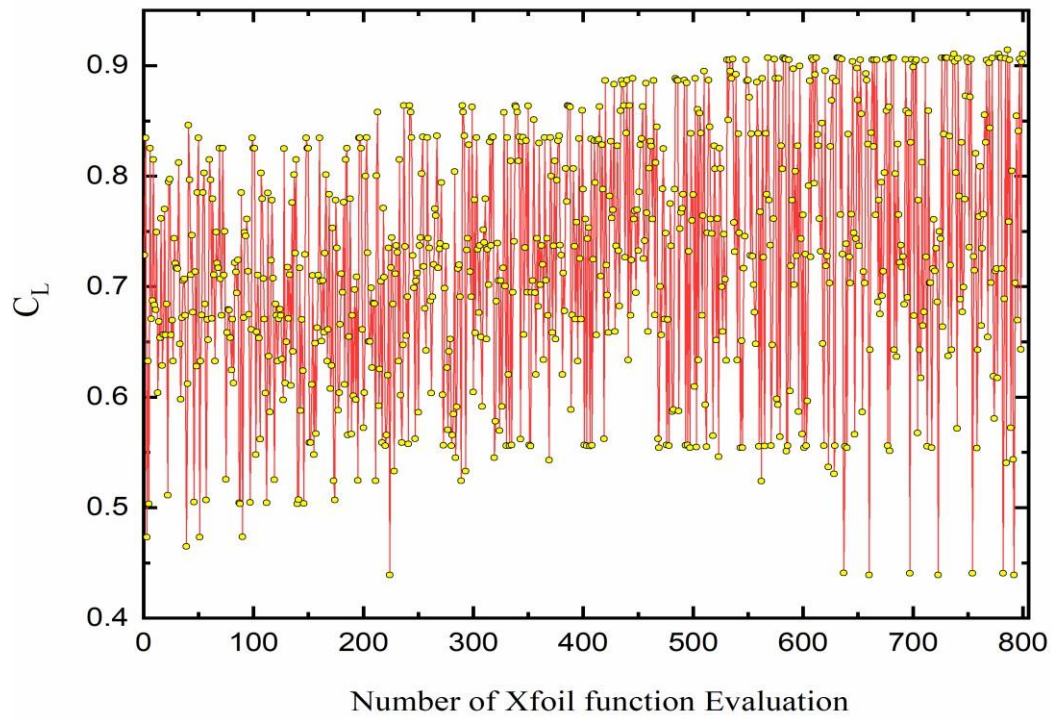
(a)
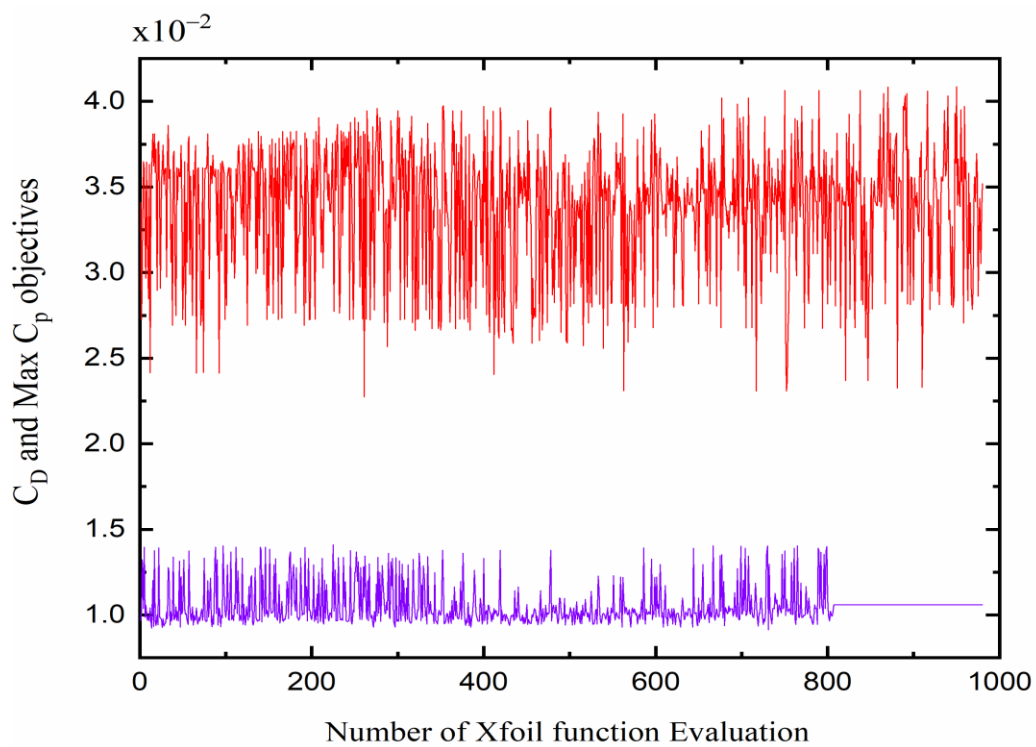
(b)

**Figure 5-2:** Each shape fitness evaluation graph (a) the coefficient of lift and (b) the coefficient of drag and pressure coefficient.

Moreover, Figure 5-3 shows the result of aerodynamic analysis obtained from the panel method technique using XFOIL, both airfoils baselines and optimized. In Figure 5-3 (a) the coefficient of the lift at different angles of attack of airfoil baselines and optimized. The baseline airfoil, stall condition was achieved at an angle of attack (AOA) of 12°. Whereas, the optimized airfoil extended to an angle of attack of 17°. The coefficient of drag comparison shows the significant reduction in the drag parameter of the optimized airfoil with variation in the angle of attack compared to base airfoil values shown in Figure 5-3 (b). It was determined, that the optimized airfoil has an improved aerodynamic property which is viable for the small horizontal axis wind turbine blade, off-design property. The wind turbine selection is based on a suitable range of lift-to-drag ratio preferably, high. It shows, the efficiency of the wind turbine to convert the incoming wind speed to generate the lift coefficient compared to the drag coefficient, the optimized airfoil has a higher lift-to-drag ratio as compared to the baseline airfoil, as shown in Figure 5-4.

(a)   **(b)**
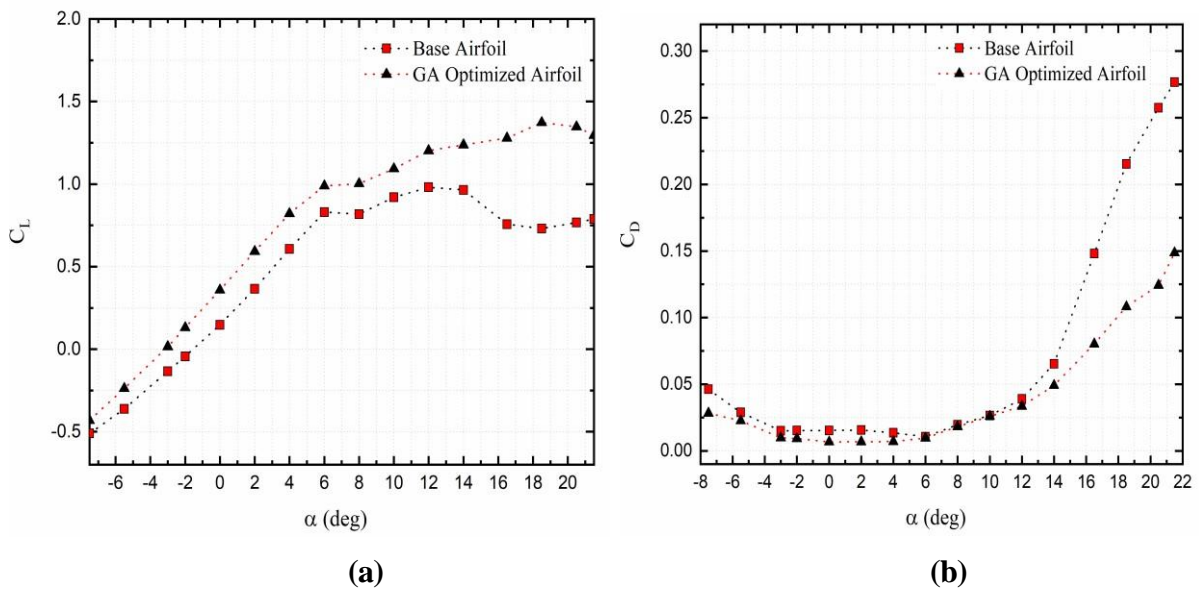
Figure 5-3: (a) Coefficient of lift concerning angle of attack. (b) Coefficient of drag concerning angle of attack.
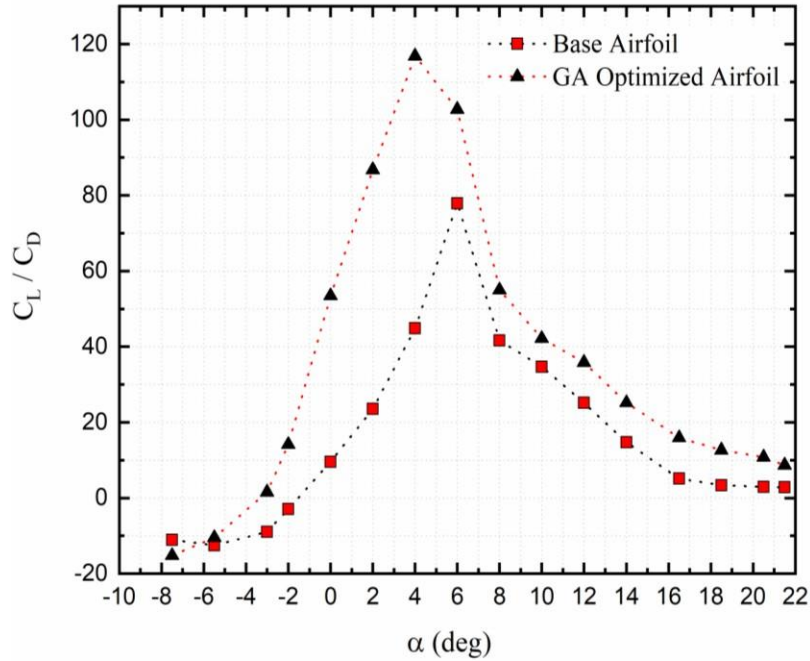
Figure 5-4: Lift-to-drag ratio concerning the angle of attack.

5.2 Numerical Validation

Figure 5-5 shows the comparison of the coefficient of the lift from experimental data of the baseline airfoil and the CFD results of the GA-optimized airfoil. A close observation shows that the optimized airfoil has a significant improvement in the coefficient of lift with a variation of the angle of attack from 0° to °10° with an interval of 2°. Airfoil shape optimization eventually benefits the blade design of a wind turbine which is an actual energy harvesting machine in wind energy. From a design perspective, 6 degrees is the most commonalty used angle of attack while designing a wind turbine. Hence a key parameter of the blade design is improved to keep at maximum level coefficient of lift and relative variation is enclosed in Table 5-2.

Table 5-2: Relative variation between experimental (baseline airfoil) and CFD (optimized airfoil) results.

Analyzed Parameters		Baseline Airfoil (Experiment [45])	Optimized Airfoil (CFD)	Relative variation (%)
AOA (6.1°)	C_L	0.731	0.930	+ 27.2
	C_D	0.012	0.013	+ 12.7
	C_L/C_D	61.95	69.92	+12.85
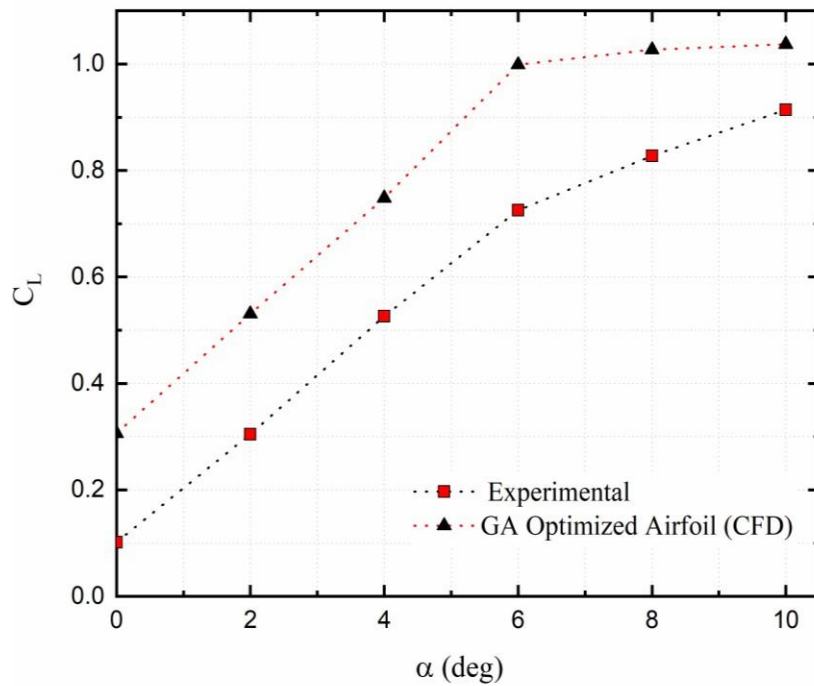
Figure 5-5: Experimental [45] and optimized (CFD) lift coefficient with angle of attack variation.
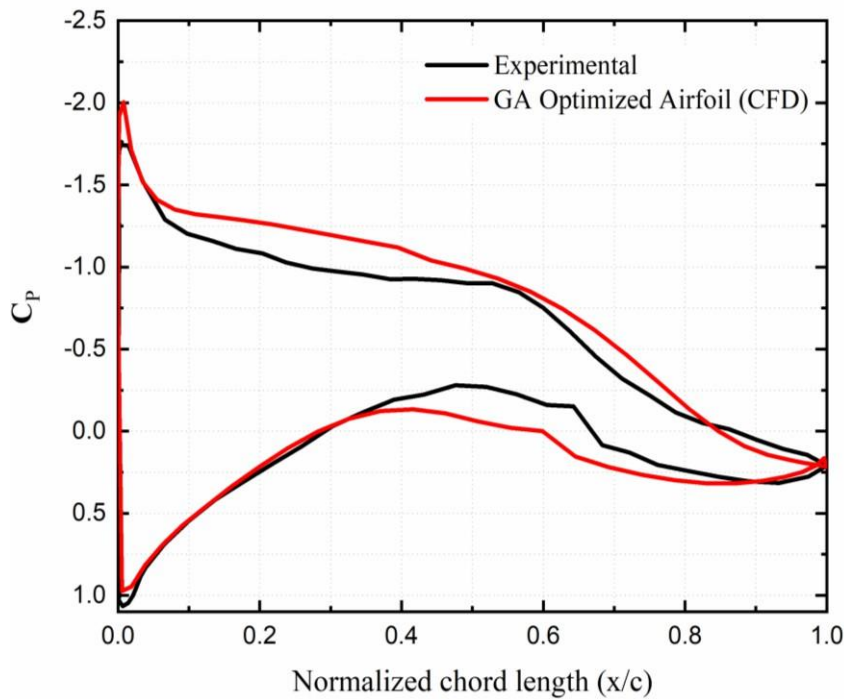
Figure 5-6: Experimental [45] and optimized Pressure distribution curve over both airfoils at AOA of 6.1°.

Figure 5-6 shows the pressure distribution curve from the leading edge to the tail edge over both the airfoil surface baseline and optimized airfoil obtained from the PARSEC method. The pressure distribution curve was obtained at the angle of attack 6.1°. The area under the curve shows the pressure difference between the curve, higher pressure at the upper surface, and lower pressure at the lower surface to generate the coefficient of lift. Experimental data shows a smaller difference as compared to optimized airfoil CFD results. At 60% of the chord length of the base airfoil, boundary layer separation can be seen. Likewise, the optimized airfoil shows a delay in boundary layer separation to avoid the flow turbulence at an angle of attack of 6.1°.

The computational fluid dynamic simulation results are visualized in Figure 5-7 and Figure 5-8 shows the static pressure distribution contour over the surface upper and lower of both airfoils baseline and optimized from the genetic algorithm. The flow conditions of the result were an inlet wind speed of $14.6 \, m/s$ and two different angles of attack 0° and 6.1°. Figures 5-7 (a), and (b) indicate the result of a base airfoil at 0° and 6.1°, respectively.

The optimized airfoil results at different angles of attack 0° and 6.1° are shown in Figure 5-8 (a) and (b) respectively. 5-8 is a piece of evidence that the pressure contour result of optimized S-810 is more in favor of aerodynamic property due to the more negative pressure over the upper surface observed as compared to the base airfoil. The generation of more lift force by optimized S-810 is the better airfoil shape in the blade design of a small horizontal axis wind turbine.
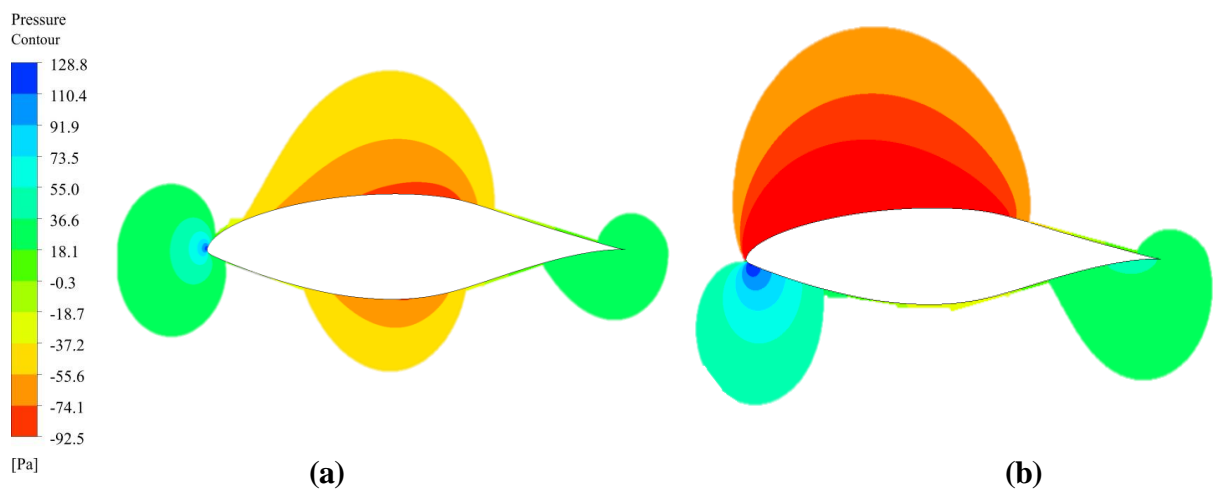
Figure 5-7: Base airfoil pressure contour at angle of attack (**a**) 0° (**b**) 6.1°.
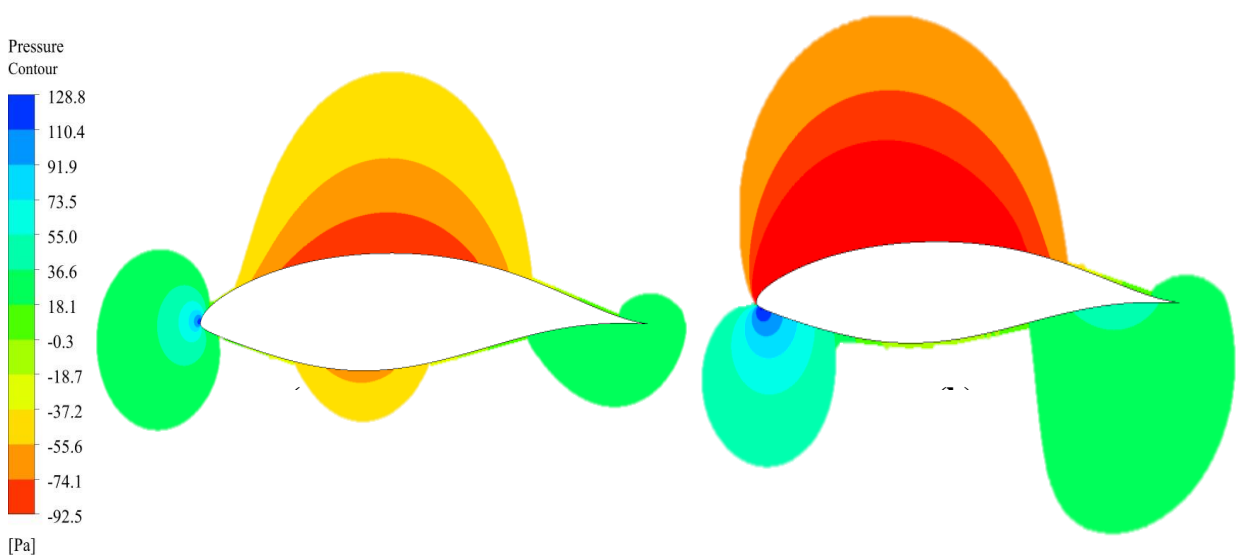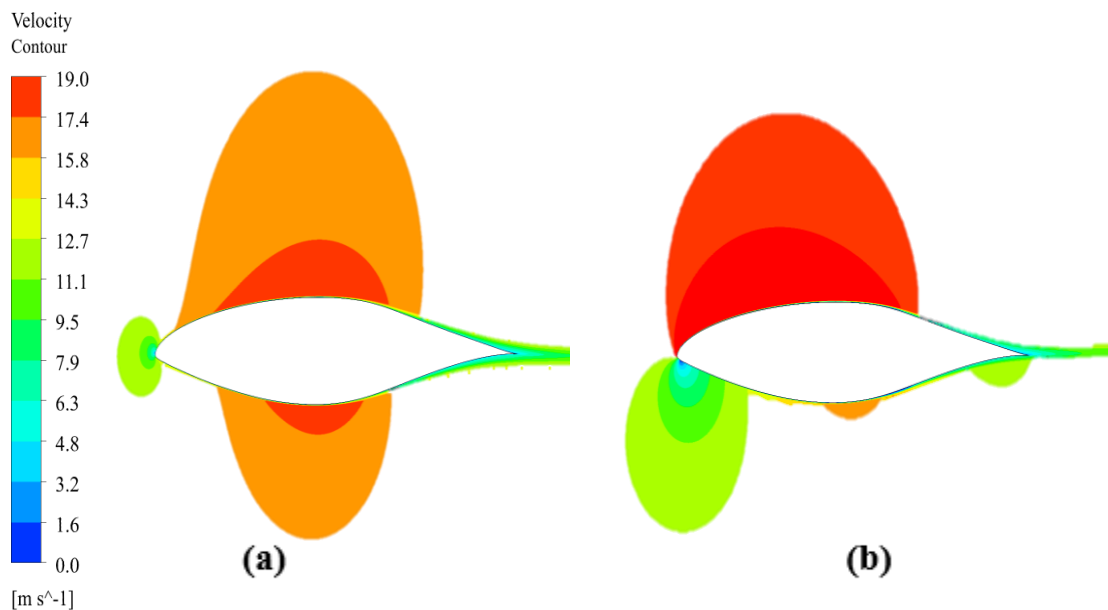

Figure 5-8: Optimized airfoil pressure contour at angle of attack (**a**) 0° (**b**) 6.1°.

Figure 5-9 represents the velocity contours over the surface of the baseline airfoil, results obtained with flow condition of wind speed $14.6\ m/s$ and two different angles of attack $0°$ and $6.1°$.

Figure 5-10 shows the optimized S-810 airfoil result of velocity contours obtained from CFD simulation at different angles of attack $0°$ and $6.1°$ as shown in Figure 5-10 (a), (b) respectively. It was observed that the stagnation point of the airfoil varies with the angle of attack, at zero on the tip of the leading edge as an increment in the angle of attack the stagnation point moves toward the lower surface of the airfoil. Similarly, the incoming velocity is higher on the upper surface as compared to the lower surface and changes with variation in the angle of attack. The other aerodynamic key parameters for the blade design including the coefficient of lift (C_L), coefficient of drag (C_D), and lift-to-drag ratio (C_L/C_D) were obtained through simulation.

From the above results and discussion, it can be determined that the optimized shape of the S-810 NREL obtained using the parameterization method PARSEC coupled with the genetic algorithm shows the same shape trend as other airfoils with improved properties of aerodynamic performance. Significantly improved results show that this methodology can be further utilized for different airfoil shapes in the process of blade design of horizontal axis wind turbines (HAWT).

Figure 5-9: Base airfoil velocity contour at angle of attack (**a**) $0°$ (**b**) $6.1°$.
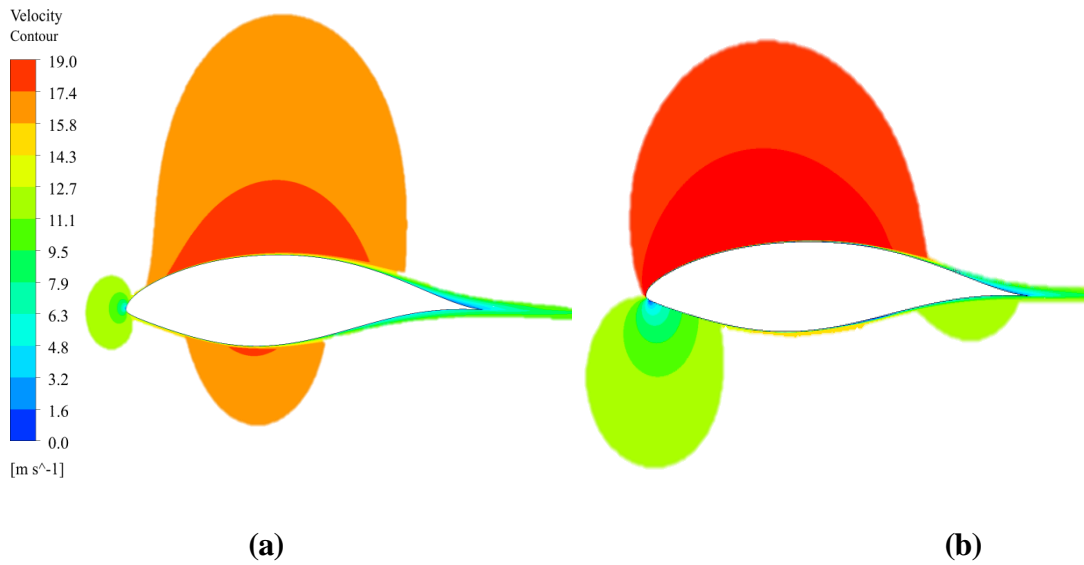
Figure 5-10: Optimized airfoil velocity contour at angle of attack (**a**) 0° (**b**) 6.1°.

Summary

This chapter provides a comprehensive presentation of steady-state simulation results performed using ANSYS FLUENT. The flow condition for the model validation used a wind speed of 14.6 m/s, a Reynolds number of 1 million, angle of attack of 6.1° with a transport shear stress model (SST). The lift coefficient and pressure coefficient of the optimized airfoil were better compared to the baseline airfoil S810. Besides, the velocity and pressure contours show the boundary layer separation over the airfoil surface at different angles of attack 0° and 6.1° of comparative analysis of both airfoils optimized and baseline.

CHAPTER 6: CONCLUSION AND FUTURE RECOMMENDATIONS

The current study has been carried out to analyze the optimization process using the parameterization method PARSEC integrated with a genetic algorithm to obtain the optimized shape of the airfoil S-810 NREL. The two key objectives of this study are successfully achieved in terms of aerodynamic property, coefficient of lift (C_L), and lift-to-drag ratio(C_L/C_D). The methodology of optimization was performed house of MATLAB, for the iterative analysis the panel method was adopted using the flow solver XFOIL, to calculate the aerodynamic property including lift, drag, and pressure distribution data. After the optimized shape CFD simulations were performed using the ANSYS FLUENT software, the structured mesh with C-type domain used for the flow field analysis with inlet wind speed $14.6\ m/s$ at two different angles of attack $0°$ and $6.1°$ combining Reynolds-averaged Navier Stokes (RANS) with two models $k-\omega$ and $k-\varepsilon$ SST turbulence model. However, a significant improvement in aerodynamic properties was noticed between the original and optimized S-810 NREL airfoil results.

The key points of conclusions are:

1. The XFOIL results of the genetic algorithm optimized airfoil, show significant improvement in lift coefficient (C_L) of 20.3% and lift-to-drag ratio(C_L/C_D) of 47.0% compared to baseline airfoil NREL S-810 at an angle of attack of 6.1 °.

2. The improvement in the off-design parameter of a small horizontal axis wind turbine, dynamic stall of the optimized airfoil extended to an angle of attack 5° from 12° to 17° comparatively, baseline airfoil.

3. To further strengthen the XFOIL result of the optimized airfoil, CFD simulation of steady-state was performed at an angle of attack 6.1°, and the relative variation was observed in lift coefficient of (C_L) 6.5% decrement and 45% increment in coefficient of drag (C_D).

4. The comparative analysis of experimental data of baseline airfoil published by Ohio State University and CFD result of optimized airfoil S-810 improved, lift coefficient of 27.2% and lift-to-drag ratio of 12.85% relatively.

This study considerably outlines a solution for airfoil optimization by following the trend of airfoil shape with improvement in aerodynamic properties helps to optimize the whole blade design for small horizontal axis wind turbines with improved flexibility off-design conditions.

REFERENCES

[1] Q. Bchini, G. Duffour, and A. Peffen, "Global Energy Climate Trends 2024 Edition," *Enerdata*, 2024, [Online]. Available: https://www.enerdata.net/publications/reports-presentations/world-energy- trends.html

[2] J. R. R. A. Martins, "Aerodynamic design optimization: Challenges and perspectives," *Comput. Fluids*, vol. 239, no. February, p. 105391, 2022, doi: 10.1016/j.compfluid.2022.105391.

[3] X. Tang, K. Yuan, N. Gu, P. Li, and R. Peng, "An interval quantification-based optimization approach for wind turbine airfoil under uncertainties," *Energy*, vol. 244, p. 122623, 2022, doi: 10.1016/j.energy.2021.122623.

[4] X. Wei, X. Wang, and S. Chen, "Research on parameterization and optimization procedure of low-Reynolds-number airfoils based on genetic algorithm and Bezier curve," *Adv. Eng. Softw.*, vol. 149, no. May, p. 102864, 2020, doi: 10.1016/j.advengsoft.2020.102864.

[5] X. Wu, W. Zhang, X. Peng, and Z. Wang, "Benchmark aerodynamic shape optimization with the POD-based CST airfoil parametric method," *Aerosp. Sci. Technol.*, vol. 84, pp. 632–640, 2019, doi: 10.1016/j.ast.2018.08.005.

[6] J. F. Herbert-Acero, O. Probst, C. I. Rivera-Solorio, K. K. Castillo-Villar, and S. Mendez-Diaz, "An extended assessment of fluid flow models for the prediction of two-dimensional steady-state airfoil aerodynamics," *Math. Probl. Eng.*, vol. 2015, pp. 6–10, 2015, doi: 10.1155/2015/854308.

[7] P. Della Vecchia, E. Daniele, and E. D'Amato, "An airfoil shape optimization technique coupling PARSEC parameterization and evolutionary algorithm," *Aerosp. Sci. Technol.*, vol. 32, no. 1, pp. 103–110, 2014, doi: 10.1016/j.ast.2013.11.006.

[8] S. N. Skinner and H. Zare-Behtash, "State-of-the-art in aerodynamic shape optimisation methods," *Appl. Soft Comput. J.*, vol. 62, pp. 933–962, 2018, doi: 10.1016/j.asoc.2017.09.030.

[9]   H. P. Buckley, B. Y. Zhou, and D. W. Zingg, "Airfoil optimization using practical aerodynamic design requirements," *J. Aircr.*, vol. 47, no. 5, pp. 1707– 1719, 2010, doi: 10.2514/1.C000256.

[10]   A. Meana-Fernández, J. M. Fernández Oro, K. M. Argüelles Díaz, and S. Velarde-Suárez, "Turbulence-model comparison for aerodynamic-performance prediction of a typical vertical-axis wind-turbine airfoil," *Energies*, vol. 12, no. 3, pp. 1–16, 2019, doi: 10.3390/en12030488.

[11]   H. W. Lim and H. Kim, "Multi-objective airfoil shape optimization using an adaptive hybrid evolutionary algorithm," *Aerosp. Sci. Technol.*, vol. 87, pp. 141– 153, 2019, doi: 10.1016/j.ast.2019.02.016.

[12]   A. F. P. Ribeiro, A. M. Awruch, and H. M. Gomes, "An airfoil optimization technique for wind turbines," *Appl. Math. Model.*, vol. 36, no. 10, pp. 4898– 4907, 2012, doi: 10.1016/j.apm.2011.12.026.

[13]   D. Jha, M. Singh, and A. N. Thakur, "A novel computational approach for design and performance investigation of small wind turbine blade with extended BEM theory," *Int. J. Energy Environ. Eng.*, vol. 12, no. 3, pp. 563–575, 2021, doi: 10.1007/s40095-021-00388-y.

[14]   P. Sharma, B. Gupta, M. Pandey, A. K. Sharma, and R. Nareliya Mishra, "Recent advancements in optimization methods for wind turbine airfoil design: A review," *Mater. Today Proc.*, vol. 47, pp. 6556–6563, 2020, doi: 10.1016/j.matpr.2021.02.231.

[15]   D. A. Masters, N. J. Taylor, T. C. S. Rendall, C. B. Allen, and D. J. Poole, "Geometric comparison of aerofoil shape parameterization methods," *AIAA J.*, vol. 55, no. 5, pp. 1575–1589, 2017, doi: 10.2514/1.J054943.

[16]   M. Science, "Turbine Blades Awsi," vol. 8694, no. 1, pp. 1–8, 2013.

[17]   V. Raul and L. Leifsson, "Multifidelity aerodynamic shape optimization for airfoil dynamic stall mitigation using manifold mapping," *J. Comput. Sci.*, vol. 75, no. March 2023, p. 102213, 2024, doi: 10.1016/j.jocs.2024.102213.

[18]   H. M. Sheikh, S. Lee, J. Wang, and P. S. Marcus, "Airfoil optimization using Design-by-Morphing," *J. Comput. Des. Eng.*, vol. 10, no. 4, pp. 1443–1459, 2023, doi: 10.1093/jcde/qwad059.

[19]   K. Wang, S. Yu, Z. Wang, R. Feng, and T. Liu, "Adjoint-based airfoil optimization with adaptive isogeometric discontinuous Galerkin method," *Comput. Methods Appl. Mech. Eng.*, vol. 344, pp. 602–625, 2019, doi: 10.1016/j.cma.2018.10.033.

[20]   Z. Zhang, Y. Ao, S. Li, and G. X. Gu, "An adaptive machine learning-based optimization method in the aerodynamic analysis of a finite wing under various cruise conditions," *Theor. Appl. Mech. Lett.*, vol. 14, no. 1, 2024, doi: 10.1016/j.taml.2023.100489.

[21]   J. Li *et al.*, "Low-Reynolds-number airfoil design optimization using deep- learning-based tailored airfoil modes," *Aerosp. Sci. Technol.*, vol. 121, p. 107309, 2022, doi: 10.1016/j.ast.2021.107309.

[22]   B. Lian, H. Yan, and J. Wang, "Performance analysis of three heuristic algorithms for airfoil design optimization," *Int. J. Green Energy*, vol. 19, no. 4, pp. 349–364, 2022, doi: 10.1080/15435075.2021.1946813.

[23]   A. Saleem and M. H. Kim, "Aerodynamic performance optimization of an airfoil-based airborne wind turbine using genetic algorithm," *Energy*, vol. 203, p. 117841, 2020, doi: 10.1016/j.energy.2020.117841.

[24]   R. C. Swanson and S. Langer, "Steady-state laminar flow solutions for NACA 0012 airfoil," *Comput. Fluids*, vol. 126, pp. 102–128, 2016, doi: 10.1016/j.compfluid.2015.11.009.

[25]   J. Bartl, K. F. Sagmo, T. Bracchi, and L. Sætran, "Performance of the NREL

S826 airfoil at low to moderate Reynolds numbers—A reference experiment for CFD models," *Eur. J. Mech. B/Fluids*, vol. 75, pp. 180–192, 2019, doi: 10.1016/j.euromechflu.2018.10.002.

[26]   A. Aprovitola, L. Iuspa, G. Pezzella, and A. Viviani, "Aerodynamic optimization of airfoils shape for atmospheric flight on Mars planet," *Acta Astronaut.*, vol. 212, no. August, pp. 580–594, 2023, doi: 10.1016/j.actaastro.2023.08.028.

[27]   J. Chen, X. Pan, C. Wang, G. Hu, H. Xu, and P. Liu, "Airfoil parameterization evaluation based on a modified PARASEC method for a H-Darrious rotor," *Energy*, vol. 187, p. 115910, 2019, doi: 10.1016/j.energy.2019.115910.

[28]   X. Liu, F. Wei, and G. Zhang, "Uncertainty optimization design of airfoil based on adaptive point adding strategy," *Aerosp. Sci. Technol.*, vol. 130, p. 107875, 2022, doi: 10.1016/j.ast.2022.107875.

[29]   A. Shahrokhi and A. Jahangirian, "Airfoil shape parameterization for optimum Navier-Stokes design with genetic algorithm," *Aerosp. Sci. Technol.*, vol. 11, no. 6, pp. 443–450, 2007, doi: 10.1016/j.ast.2007.04.004.

[30]   Q. S. Ali and M. H. Kim, "Design and performance analysis of an airborne wind turbine for high-altitude energy harvesting," *Energy*, vol. 230, p. 120829, 2021, doi: 10.1016/j.energy.2021.120829.

[31]   J. Slotnick, A. Khodadoust, J. Alonso, and D. Darmofal, "CFD Vision 2030 Study: A Path to Revolutionary Computational Aerosciences," *Nnasa/Cr-2014- 218178*, no. March, 2014.

[32]   H. Sobieczky, "Parametric Airfoils and Wings, Notes on Numerical Fluid Mechanics," vol. 68, pp. 71–87, 1999.

[33]   V. Raul and L. Leifsson, "Multifidelity aerodynamic shape optimization for airfoil dynamic stall mitigation using manifold mapping," *J. Comput. Sci.*, vol. 75, no. December 2023, p. 102213, 2024, doi: 10.1016/j.jocs.2024.102213.

[34]   D. E. Goldberg and K. Deb, *A Comparative Analysis of Selection Schemes Used in Genetic Algorithms*, vol. 1. Morgan Kaufmann Publishers, Inc., 1991. doi:

10.1016/b978-0-08-050684-5.50008-2.

[35]   H. C. Ayazümütlü and Z. Kiral, "Airfoil Shape Optimization Using Bézier Curve and Genetic Algorithm," *Aviation*, vol. 26, no. 1, pp. 32–40, 2022, doi: 10.3846/aviation.2022.16471.

[36]   K. R. Ram, S. P. Lal, and M. R. Ahmed, "Design and optimization of airfoils and a 20 kW wind turbine using multi-objective genetic algorithm and HARP_Opt code," *Renew. Energy*, vol. 144, pp. 56–67, 2019, doi: 10.1016/j.renene.2018.08.040.

[37]   J. Caron and J. R. Markusen, Introduction to Genetic Algorithm. 2016.

[38]   P. Diaz-Gomez and D. Hougen, "Initial Population for Genetic Algorithms: A Metric Approach.," *Proc. 2007 Int. Conf. Genet. Evol. Methods*, no. January 2007, pp. 43–49, 2007.

[39]   J. D. Dyer and R. J. Hartfield, "Aerospace Design Optimization Using a Steady State AIAA-2008-5921-467.pdf," no. September, 2008.

[40]   M. Nemati and A. Jahangirian, "Robust aerodynamic morphing shape optimization for high-lift missions," *Aerosp. Sci. Technol.*, vol. 103, p. 105897, 2020, doi: 10.1016/j.ast.2020.105897.

[41]   X. Chen and R. K. Agarwal, "Optimization of wind turbine blade airfoils using a multi-objective genetic algorithm," *J. Aircr.*, vol. 50, no. 2, pp. 519–527, 2013, doi: 10.2514/1.C031910.

[42]   C. Alkalah, Soft Computing in Engineering Design and Manufacturing, vol. 19, no. 5. 2016.

[43]   "David E. Goldberg - Genetic Algorithms in Search, Optimization, and Machine Learning-Addison-Wesley Professional (1989).pdf."

[44]   I. ANSYS, "CFD Experts Simulate the Future," 2021, [Online]. Available: https://www.ansys.com/

[45]   M. J. Hoffmann, R. Reuss Ramsay, and G. M. Gregorek, "Effects of grit roughness and pitch oscillations on the NACA 4415 airfoil," *Nrel/Tp-442-7817*, no. December,

p.152, 1996, [Online]. Available: http://www.osti.gov/servlets/purl/266691-Iy1spR/webviewable/

List Of Publication

Full-length article title: Optimization of Wind Turbine Airfoil NREL S-810 for Improving Lift and Efficiency Using AI-Based Approach

Journal: Wind Engineering & Industrial Aerodynamics

Impact Factor: 4.2, Q1 Index

Manuscript number: INDAER-D-24-00876

Date of submission: 1st November 2024

Current Status: With Editor (09 December 2024)

Action ☐ ▽⚡	Manuscript Number ▲	Title ▲	Initial Date Submitted ▼	Status Date ▲	Current Status ▲
View Submission Send E-mail	INDAER-D-24-00876	Optimization of Wind Turbine Airfoil NREL S-810 for Improving Lift and Efficiency Using AI Based Approach	Nov 01, 2024	Nov 01, 2024	With Editor